Short title: Isoprene, cytokinins, leaf and plant senescence

Authors for contact details: Kaidala Ganesha Srikanta Dani, Francesco Loreto

Article title

Isoprene enhances leaf cytokinin metabolism, accelerates growth and induces early-senescence in *Arabidopsis* and *Populus*

Kaidala Ganesha Srikanta Dani[1,6*], Susanna Pollastri[1], Sara Pinosio[2], Michael Reichelt[3], Thomas D Sharkey[4], Jorg-Peter Schnitzler[5], **Francesco Loreto**[6*]

[1] Institute for Sustainable Plant Protection, National Research Council of Italy, Via Madonna del Piano 10, Sesto Fiorentino 50019, Florence, Italy

[2] Institute of Biosciences and Bioresources, National Research Council of Italy, Via Madonna del Piano 10, Sesto Fiorentino 50019, and Institute for Applied Genomics, Udine, Italy

[3] Department of Biochemistry, Max Planck Institute for Chemical Ecology, Hans-Knöll Strasse 8, D-07745 Jena, Germany

[4] MSU-DOE Plant Research Laboratory, Department of Biochemistry and Molecular Biology, Michigan State University, East Lansing, MI 48824, USA

[5] Research Unit Environmental Simulation, Institute of Biochemical Plant Pathology, Helmholtz Zentrum München, German Research Center for Environmental Health, 85764, Neuherberg, Germany

[6] Department of Biology, Agriculture and Food Sciences, National Research Council of Italy, Piazzale Aldo Moro 7, 00185 Rome, Italy

*Corresponding authors

One sentence summary

Isoprene emission enhances leaf cytokinin abundance, hastens leaf senescence and shortens plant generation time.

List of author contributions

KGSD conceived the hypothesis, designed, led, and conducted the study with inputs from FL. TDS and JPS provided the transgenic *Arabidopsis* and poplar lines respectively. SPO helped raising the Arabidopsis seed stock and with logistics. MR extracted and quantified cytokinins. SPI assembled the RNA-seq raw reads and the transcript abundance data. KGSD monitored leaves from emergence to their full senescence course, quantified leaf photosynthesis, chloroplast energy status, leaf and plant phenotype, analysed hormonal and differential gene expression data. KGSD wrote and revised the manuscript with inputs from all authors.

Funding information

This work was fully supported by the EU Horizon2020 programme via the Marie Curie fellowship to KGSD under the grant Leaf-of-Life (2016, 746821) to FL.

Email addresses for contact:

srikantadani@yahoo.co.uk; francesco.loreto@cnr.it

Isoprene enhances leaf cytokinin metabolism, accelerates growth and induces early-senescence in *Arabidopsis* and *Populus*

Abstract

Isoprene, a volatile hemiterpene, and cytokinins (CKs), a major class of hormones, are synthesized from dimethylallyl diphosphate via the methylerythritol phosphate pathway in the chloroplast. Isoprene can impart photosynthetic stability under transient abiotic stresses but isoprene's constitutive function remains contested. We hypothesized that isoprene affects CK synthesis and potentially also influences developmental processes, gene expression, leaf and plant phenotype and senescence, all of which are critically regulated by CK-mediated signalling and transcriptional regulation. We found that naturally isoprene-emitting poplars (*Populus x canescens*) and transgenic *Arabidopsis thaliana* engineered to emit isoprene grew at a significantly greater rate compared to poplars where isoprene synthesis was suppressed by RNAi and naturally non-emitting *Arabidopsis*. Isoprene-emitting *Arabidopsis* developed bigger, fewer and significantly early senescing leaves, flowered significantly sooner and showed a shorter lifecycle duration than non-emitting controls. Isoprene-emitting poplar leaves showed higher net photosynthesis, invested significantly less photochemical energy in photorespiration, and again had shorter lifespan compared to isoprene-supressed leaves. Isoprene emission significantly enriched leaf CK-ribosides and active CK-freebases in healthy mature leaves of both *Arabidopsis* and poplar. RNA-seq identified significant enrichment of transcripts coding for *LOG* genes (*LONELEY GUY,* CK synthesis and activation), *CKX* genes (cytokinin dehydrogenases involved in CK degradation), and genes coding for response regulators involved in CK-signal transduction, all indicating greater CK activity and turnover in presence of isoprene. Transcripts of *CONSTANS-LIKE 9 (COL9)* and *EARLY FLOWERING* (*ELF3/4*), both known to be key negative regulators of flowering time, were significantly depleted in isoprene-emitting *Arabidopsis* and poplar. Acceleration of plant growth and leaf senescence, bigger leaf phenotype, stronger apical dominance (poplar), early flowering and faster completion of lifecycle (*Arabidopsis*) due to isoprene emission reveals a significant new role for isoprene in shaping plant life-history strategy mainly through isoprene-led enhancement of cytokinin availability, activity, and turnover in leaves and potentially in other plant parts.

Key words

isoprene, cytokinins, apical dominance, *LOG, CKX, ELF3,* flowering time, chloroplast energy status, methylerythritol phosphate pathway, leaf senescence, photosynthesis, reproduction, leaf senescence

Introduction

Isoprene is the most abundant biogenic volatile hydrocarbon in the atmosphere. More than 500 Tg of carbon is emitted in the form of isoprene annually by forest trees, with important consequences for global climate (Guenther et al. 2006; Mcfiggans et al. 2019). Foliar isoprene emission is shown to enhance photosynthetic stability in leaves under transient abiotic stresses such as heat (Behnke et al. 2007, Velikova et al. 2011; Pollastri et al. 2014), oxidative stress (Loreto et al. 2001; Vickers et al. 2009; Behnke et al. 2010), and drought (Dani et al. 2014a; Velikova et al. 2016). Isoprene is also viewed as a metabolic outlet for excess carbon from photosynthates, adding to the pool of photoprotective molecules (e.g. Penuelas and Munné-Bosch, 2005). The described benefits of isoprene are often apparent in plants only when they are under stressful, sub-optimal conditions. The ecological and functional relevance of isoprene emission in unstressed plants is unknown. Even the link with photosynthesis, a presumed *sine qua non*, appears tenuous in unicellular heterotrophic eukaryotes that can emit appreciable levels of isoprene in complete darkness (Dani et al. *under review*). Finally, the evolutionary history of constitutive isoprene emission across the tree of life has remained unresolved (Monson et al. 2013; Dani et al. 2015a).

The plastid-localised methylerythritol phosphate (MEP) pathway not only makes isoprene but also acts as a source of vital plant hormones including cytokinins (CKs) (such as isopentenyladenine and zeatin), abscisic acid, and accessory photosynthetic and photoprotective pigments such as β-carotene and xanthophylls, all of which directly regulate and influence leaf senescence (Dani et al. 2016). CKs are critically required for leaf development and expansion (e.g. Werner et al. 2001), and for the modulation of expression of transcription factors in regulating abiotic stress response, prevention of chlorophyll decay and maintenance of chloroplast integrity (Zavaleta-Mancera et al. 2007, Nishiyama et al. 2011; Cortleven and Schmülling, 2015; Raines et al. 2016). In the MEP pathway, dimethylallyl diphosphate (DMADP) is combined with adenosine triphosphate (ATP) to give iP-type CKs by isopentenyl transferase (IPT, Kasahara et al. 2004; Sakakibara et al. 2006), whereas DMADP is converted to isoprene by isoprene synthase (Sharkey and Yeh, 2001). Overexpression of *IPT* by a promoter of

senescence-associated genes is an established way of delaying leaf senescence (Guo and Gan, 2014). Overexpression of isoprene synthase and even exogenous isoprene has been shown to modulate gene expression in unstressed plants (Harvey and Sharkey, 2016; Zuo et al. 2019), although any influence of isoprene on the process of leaf and plant senescence remain untested. Isoprene emission capacity has evolved frequently in fast-growing perennial tree genera that are generally hydrophytic and highly speciose (Dani et al. 2014b; Loreto et al. 2014), potentially via neofunctionalization of monoterpene synthases (Dani et al. 2014b; Li et al. 2017). In this context, we had proposed that the entire MEP pathway in the chloroplast, along with isoprene, is under selection to regulate leaf senescence (Dani et al. 2016). We premised that leaf senescence sets a limit to isoprene emission, and that isoprene acts along with cytokinins and other isoprenoid hormones to regulate leaf senescence.

Naturally isoprene-emitting poplar trees (*Populus* spp.) have served as the model system for isoprene-related research for a couple of decades (e.g. Schnitzler et al. 2005; Behnke et al. 2007; Monson et al. 2020). Some insights have also come from transgenic isoprene-emitting *Arabidopsis thaliana* (e.g. Sasaki et al. 2007; Loivamäki et al. 2007; Vickers et al. 2011; Zuo et al. 2019). By model systems of *Arabidopsis* lines transformed with a eucalypt isoprene synthase to emit isoprene, and grey poplar (*Populus x canescence*) lines genetically modified (by RNA-interference) to suppress isoprene synthase activity and isoprene emission, we comprehensively quantified the impact of isoprene emission on developmental plant phenotype, growth rate, and leaf senescence trajectories. We also modelled photosynthetic energy status of individual leaves from emergence until abscission, detected and quantified the changes in the abundance of leaf CKs in presence and absence of isoprene, and examined the genome-wide impact on poplar and *Arabidopsis* transcriptome by RNA-seq. Our results highlight novel functional possibilities for isoprene in shaping leaf phenotype and lifespan, revealing new evolutionary and adaptive significance of isoprene emission.

Materials and Methods

Plant material

Arabidopsis: Isoprene-emitting transgenic *Arabidopsis* lines were generated at the plant transformation

facility in Michigan State University (Zuo et al. 2019). The cloning construct included the complete CDS of isoprene synthase (ISPS) from *Eucalyptus globulus* downstream to the Arabidopsis Rubisco SSU promoter rbcS-1A. Another construct lacking ISPS was used as the empty vector control. *Arabidopsis* Col-0 were transformed using Agrobacterium via the floral dip method. Seven independent transgenic lines were obtained (selected on kanamycin) until F3 transgenic seeds were obtained and verified by PCR. We selected two transformants and one empty vector line for this intensive study, based on preliminary observations (now given in Zuo et al. 2019). Seeds of *Arabidopsis thaliana* wildtype control (ecotype Col-0), empty vector control (line EV-B3), and two isoprene-emitting lines (ISPS-B2 and ISPS-C4) were deposited at the Arabidopsis Biological Resource Center in Ohio State University, USA and formally obtained in Italy. Seeds were surface sterilized in 70% ethanol, transferred to petri plates containing Murashige and Skoog's agar medium, and vernalized at 4 °C for 48 h. Plates were then transferred to a growth cabinet and allowed to germinate at 18 ± 2 °C, long days (16 h day: 8 h night), light intensity of 100 µmol m^{-2} s^{-1} from white fluorescent tubes, and 40% relative humidity. Seedlings were individually transplanted to soil-substrate containers placed in plastic trays and watered regularly. Inflorescence and pods were allowed to dry naturally while attached to the plants, and seeds were harvested. An independent set of plants of the four lines were grown under a light intensity of 200 µmol m^{-2} s^{-1}, constituting high-light treatment (all other conditions remaining identical to those used during seed germination).

Poplar: Isoprene-emitting wildtype Grey poplars (*Populus x canescens*) along with two transgenic lines in which expression of isoprene synthase (*PcISPS*) was suppressed by RNA-interference were used. Transgenics were generated and micropropagated at the Institute of Biochemical Plant Pathology, Helmholtz Centre in Munich (Germany). RNA*i*-mediated post transcriptional silencing of isoprene synthase in poplars was enabled by the introduction of sense and antisense hairpin sequences (160 bp, highly specific to isoprene synthase) in a binary vector via *Agrobacterium* mediated transformation (35S:PcISPS-RNA*i*; Behnke et al. 2007). Rooted 3-month-old cuttings (15 individuals each of wild type (WT), Empty Vector (EV), RA1 and RA2 isoprene-suppressed lines) were brought to the National Research Council (CNR) research area in Florence (Italy). The saplings were initially grown in 2 L pots containing soil substrate (25%), silica sand (25%), perlite (50% v/v) and slow release fertilizer. Young

saplings were soon transplanted to 7 L pots (for 2 months) and later transplanted to 18 L pots with the same soil substrate. Poplars were watered regularly and acclimated to natural seasonal variation in sun light intensity, photoperiod, temperature, and humidity in a CNR experimental facility for genetically modified organisms. After the first season (from April 2018 until December 2018), the main stems were pruned to get stubs (1.5 m) without any leaves or branches. These rooted-stem cuttings from year 1 were transferred to 40 L pots in February of year 2. Budbreak commenced in March, and the second seasonal monitoring of leaf development and senescence went on until December 2019. The microclimate data in the experimental site for the two years of the experiment was gathered from the weather monitoring and modelling centre maintained by Consorzio LaMMA of CNR.

Plant developmental phenotyping

Arabidopsis: The day *Arabidopsis* seeds germinated was noted day 0. Leaf samples were collected at six time points during the plant's lifecycle, classified on the basis of days after germination (DAG) and flowering. Leaves were numbered according to their order of emergence from base to apex, excluding cotyledon leaves. Leaves in position 7, 8, 9, and 10 from the base (the biggest leaves) were marked. A first batch of plants was grown under the same light intensity at which plants germinated (100 µmol photons m^{-2} s^{-1}). For this batch, leaves were sampled at 28 DAG (youngest stage sampled), 36 DAG (leaves 7 and 8 fully expanded), 48 DAG (fully mature plant body, prior to bolting), 56 DAG (early-senescence phase, inflorescence seen in all four lines), 64 DAG (mid-senescence phase), and finally at 76 DAG (late-senescence phase, near-end of lifecycle). Inflorescence was cut and weighed at 56, 64 and 76 DAG. A second batch of *Arabidopsis* plants were grown under 200 µmol photons m^{-2} s^{-1}, and leaves in positions 7, 8, 9, and 10 were sampled at 24, 28, 36, and 48 DAG respectively.

Poplar: Poplar leaves were tagged at the time of emergence. Leaves were grouped into three categories. (1) Spring leaves (emerging in May and later constituting the lower leaves of the main stem) (2) Summer leaves (emerging July and representing the intermediate leaves of the stem), and (3) Autumn leaves (emerging in September and representing the apical leaves of the stem, at the end of the season). Leaf area was measured using a LI-3000 portable area meter (LI-COR Biosciences Inc., USA). Apical extension was measured once every fortnight to once a month, and sub-seasonal trends in apical growth

rate were calculated. At the end of growing season, branching pattern was quantified by marking the branches (from base to apex) and by measuring their length and fresh weight post-harvest.

Measurements of gas exchange and calculation of energy status and kinetic parameters

Arabidopsis: Net photosynthesis (P_n), stomatal conductance (g_s), transpiration rate (T_r), and intercellular CO_2 concentration (C_i) were measured on fully expanded leaves in positions 8 to 12 (N=5 individual plants) before flowering (40 to 48 DAG) and after flowering (64 to 72 DAG). Measurements were made between 11 am and 3 pm, using a LICOR 6400 infrared gas analyser (LI-COR Biosciences Inc., USA). Leaves clamped in the circular leaf cuvette (area: 2 cm^2) were maintained at 20 °C, light intensity was set to 150 µmol m^{-2} s^{-1} for low-light acclimated plants and 250 µmol m^{-2} s^{-1} for high-light acclimated plants, volatile-free clean air was humidified to achieve ~40% RH (leaf to air vapour pressure deficit was 0.9 to 1.2 kPa) and CO_2 concentration was 400 µmol mol^{-1}.

Poplar. In poplar leaves, all gas exchange measurements were carried out using a LI-COR 6400XT between 10 am and 3 pm, on bright sunny days, and on individual leaves at three to four stages of a leaf lifecycle (see above). Leaf temperature was 24 ± 1 °C in April, 28 ± 1 °C in June/July, 24 ± 1 °C in September/October, and 20 ± 1 °C in November/December. In all measurements the relative humidity was maintained between 40 and 65%, and the light intensity was set to 1500 µmol m^{-2} s^{-1} (except for leaves senescing in Nov/Dec, when light intensity was set to 1000 µmol m^{-2} s^{-1}).

Photosynthesis response to increases and decreases in CO_2 concentration was recorded in poplar leaves throughout their lifecycle. V_{cmax} (maximum carboxylation rate of Rubisco) and J (instantaneous electron transport rate) were estimated by fitting net assimilation rate (P_n) vs. C_i curves using excel based curve-fitting tools (e.g. Sharkey. 2016; Bellasio et al. 2016). The chloroplast energy status of the leaves was quantified using the following equations:

$$R_l = \frac{1}{12}[J - 4\,(P_n + R_d)] \quad (1)$$

$$J_c = \frac{1}{3}\,[J + 8\,(P_n + R_d)\,] \quad (2)$$

$$J_o = \frac{2}{3}\,[J - 4\,(P_n + R_d)\,] \quad (3)$$

$$V_o = \frac{1}{6}\,[J - \frac{2}{3}(P_n + R_d)\,] \quad (4)$$

218 $$V_c = (P_n + R_d) + \frac{1}{2}V_o \quad (5)$$

Term	Description
P_n	Net rate of CO_2 uptake per unit of projected leaf area (μmol m^{-2} s^{-1})
C_i	Intercellular CO_2 concentration (μmol mol^{-1})
J	Instantaneous electron transport rate (μmol e^- m^{-2} s^{-1})
J_c	Proportion of J utilised for carboxylation of RuBP by Rubisco
J_o	Proportion of J utilised for oxygenation of RuBP by Rubisco (photorespiration)
K_m	Effective Michaelis-Menten coefficient for carboxylation by Rubisco (at 25 ˚C)
R_d	Day mitochondrial respiration rate (μmol m^{-2} s^{-1})
R_l	Photorespiration rate (μmol m^{-2} s^{-1})
V_{cmax}	Maximum rate of RuBP carboxylation by Rubisco (μmol m^{-2} s^{-1})
V_c	Rate of carboxylation by Rubisco
V_o	Rate of oxygenation by Rubisco

219

220 **Measurements of imaging chlorophyll fluorescence**

221 The maximal quantum yield of chlorophyll fluorescence (F_v/F_m) and the electron transport rate were
222 estimated by chlorophyll fluorescence imaging using a Walz Imaging PAM (Heinz Walz, Germany).
223 For *Arabidopsis* grown in low light (100 μmol m^{-2} s^{-1}) whole plants (<28 DAG) and leaves cut from
224 fully mature plants (>42 DAG, except WT line) were used during imaging. In poplars, individual cut
225 leaves were sampled at 30, 60, 90, 120, and 180 days after emergence (DAE) and used for fluorescence
226 measurements. All leaves were dark-adapted for 30 min before imaging.

227

228 **Isoprene sampling and quantification**

229 Isoprene sampling was done from fully expanded leaves in position 9, 10, 11, and 12 (between stage 2
230 and 3) for Arabidopsis, and fully mature spring, summer, and autumn leaves of poplars. A portion (300
231 mL min^{-1}) of the LI-COR cuvette outflow was diverted using a mass flow pump (AC Buck Inc. FL,
232 USA) onto a cartridge filled with absorbents (30 mg each of Carbosieve X and Carbosieve B, Supelco,
233 USA). Isoprene from emitting lines was quantified using thermal desorption gas chromatography-mass
234 spectrometry (after Dani et al. under review). Briefly, an Agilent 5975 gas chromatograph-mass
235 spectrometer (GC-MS) system was fitted with an HP-INNOWax (50 m length, 0.2 mm ID, 0.4 μm film)
236 column. Thermal desorption was executed by a Twister® multipurpose autosampler and TD unit
237 (Gerstel Technologies, Germany) fitted with an e-Trap cryofocussing system (Chromtech, Germany).
238 The GC separation programme was 40 ˚C for 1 min, reaching 110 ˚C at 5 ˚C min^{-1}, held for 10 min, and

239 then increased to 260 ˚C at 30 ˚C min^{-1} and held for 2 min. Isoprene standards were prepared in 2 L
240 Tedlar bags (Sigma-Aldrich, USA) containing nitrogen, and analysed as above. Samples collected from
241 the cuvette headspace containing control lines were treated as zero-isoprene controls.
242
243 **Extraction and quantification of cytokinins**
244 Cytokinins (CKs) were extracted from leaves harvested in positions 7 to 10 (sampled at 28, 36 and 48
245 DAG) in *Arabidopsis*, and from spring, summer and autumn leaves of poplars at different stages of leaf
246 lifecycle (soon after emergence, 60 and 90 days after emergence, and during late phases of senescence).
247 CKs were extracted in acidified aqueous methanol, purified by two solid-phase extraction (SPE) steps
248 and subsequently measured with LC-MS/MS (after Schäfer et.al. 2014). Briefly, 30 to 400 mg ground
249 plant tissue was extracted twice with 800 µL MeOH:H_2O:HCOOH (15:4:1) at −20 °C. Deuterated
250 internal CK standards in the form of 0.2 ng [$^2H_6$] IPR, 0.2 ng [$^2H_5$] tZR, and 1 ng [$^2H_5$] tZ were
251 supplemented in the first extraction step (standards from OlChemIm s.r.o., Czech Republic). Extraction
252 and SPE were performed in 96 Well BioTubes (Arctic White LLC) and 96-Well Deep Well Plates
253 (Thermo Scientific). The first SPE step was performed on a Multi 96 HR-X column (Macherey-Nagel,
254 www.mn-net.com/us/chromatography/) conditioned with extraction buffer. The flow through was
255 collected and the MeOH was evaporated at 42 °C under constant nitrogen flow. Then, 850 µL of 1 M
256 HCOOH was added to the samples and loaded on a Multi 96 HR-XC column (Macherey-Nagel) pre-
257 conditioned with 1 M HCOOH. Sequentially 1 mL each of 1 M HCOOH, MeOH, 0.35 M NH_4OH were
258 added and eluted. Finally, CKs were eluted with 1 mL 0.35 M NH_4OH in 60% MeOH. The second SPE
259 was performed using a Chromabond Multi 96 vacuum chamber. After evaporation, samples were
260 reconstituted in 50 µL 0.1% acetic acid (after Zhang et.al. 2016). CKs were chromatographically
261 separated on a Zorbax Eclipse XDB-C18 column (50×4.6 mm, 1.8 µm) at 25 °C fitted to an Agilent
262 1200 HPLC system (Agilent Tech, USA). Solvent A (water, 0.05% HCOOH) and solvent B
263 (acetonitrile) mixture was suppled at 1.1 mL min^{-1} [0 to 0.5 min, 95% A; 0.5 to 5 min, 5 to 31.5% B in
264 A; 5 to 6.5 min, 100% B; and 6.5 to 9 min 95% A]. The LC was coupled to an API 6500 tandem mass
265 spectrometer (AB Sciex, Germany) equipped with a Turbospray ion source and quadrupole mass

analyser. The MS was in positive ionization mode (MRM modus) to monitor analyte parent to product ion conversion (Table S1). Data was acquired and processed using Analyst 1.6.3 software (AB Sciex).

RNA extraction, library preparation, RNA-seq and differential gene expression analysis

Fully-expanded *Arabidopsis* leaves in position 8, 9, 10 (from the base) were sampled from 8 individuals per each line before flowering i.e., 36 to 40 days after germination (DAG) under low-light treatment, and 28 to 36 DAG under high-light treatment. Summer leaves from poplars were sampled from four individuals (per line) at 60 and 90 days after emergence (DAE). Leaves were frozen in liquid nitrogen and stored at −80 °C. *Arabidopsis* leaves were pooled (2 to 3 individuals forming one biological replicate) to get sufficient starting material for RNA extraction. Leaves from two *Arabidopsis* lines (non-emitting EV-B3 control and isoprene-emitting ISPS-C4) and two poplar lines (emitting WT control and isoprene-suppressed RA1) were selected for RNA-seq. Sampled leaves were ground in liquid nitrogen and total RNA was extracted from approximately 100 mg of ground leaf material (three biological replicates per genotype, per leaf life-stage) using the mirPremier Isolation Kit (Sigma-Aldrich) following the manufacturer's instructions. Ribosomal RNA depleted strand-specific RNA libraries were generated (in triplicate) using the Illumina TruSeq Stranded Total RNA library preparation kit with Ribo-Zero Plant (Illumina Inc., San Diego, CA, USA). Libraries were quantified using Agilent 2100 Bioanalyzer RNA assay (Agilent Technologies, Santa Clara, CA), pooled in equimolar amount and sequenced on a single lane on the Illumina NovaSeq 6000 sequencer to get 150 bp paired-end reads (2×15 million total reads). Images from the instruments were processed following the manufacturer's software pipeline to generate FASTQ sequence files.

Adaptor sequences and low quality 3' ends were removed from short reads using respectively CUTADAPT (Martin, 2011) and ERNE-FILTER (Del Fabbro et al. 2013). After trimming, only pairs with both reads longer than 50 bp were retained. Trimmed reads were aligned against the *Populus tremula* v2.2 reference genome (ftp://plantgenie.org/Data/PopGenIE/Populus_tremula/v2.2) and the *A. thaliana* (TAIR10) reference genome (http://www.arabidopsis.org) using STAR v2.7.2b (Dobin et al. 2013) with default parameters. The htseq-count python utility (Anders et al., 2015) was used to calculate gene-based read count values considering only uniquely mapping reads. The HTSeq count data were

used as the input to measure differential gene expression using the Bioconductor package DESeq2 v1.14.1 (Love et al. 2014) implemented in R. The raw counts of each gene were normalized to adjust for different sequencing depths across samples.

Statistical analysis

Normality of observed values (within lines) was tested using the Kolmogorov-Smirnov test. Differences in means among lines for net photosynthesis, electron transport rate, stomatal conductance, above ground biomass, and inflorescence weight (only *Arabidopsis*) were tested by one-way analysis of variance (ANOVA) followed by a post-hoc Tukey's multiple comparison test ($N \geq 10$ biological replicates per line, $\alpha=0.05$). Differences in poplar photosynthesis and chloroplast energy status were tested using data collected from >5 leaves per individual at each sampled leaf age ($N \geq 6$ biological replicates per line). Differences in isoprene emission rate and cytokinin abundance was verified by either Kruskal-Wallis *H* test for comparing medians ($N \geq 4$; $\alpha=0.05$) or by Games-Howell test for comparing means when variances were unequal ($N \geq 4$; $\alpha=0.05$, for *F* stats from ANOVA see Tables S2 to S4). Differentially expressed genes (from DESeq) were identified using pairwise comparisons at an adjusted *p*-value (FDR) threshold of ≤ 0.01 for determining significance. Transcripts with $\log_2$[fold change] > +1.5 and <–1.5 at $p_{adj} < 0.001$ were considered biologically significant, truly sensitive to presence or absence of isoprene, and shortlisted for functional interpretation. The foldchange heatmap was generated using the open source Morpheus (https://software.broadinstitute.org/morpheus) matrix visualization application. All other statistical tests were carried out using Minitab 18.1 statistical package (Minitab Inc, USA).

Results

Leaf and plant developmental phenotype

<u>*Arabidopsis:*</u> The above-ground biomass increased at a significantly greater rate during early developmental stages in isoprene-emitting *Arabidopsis* lines than in the non-emitting controls under both light regimes (Fig. 1A, 1D, see Table S2 for *F* statistics). Both ISPS-B2 and C4 lines started to bear flowers significantly sooner than non-emitting controls, and completed inflorescence growth by

64 DAG, while the non-emitting controls showed inflorescence growth until 76 DAG (Fig. 1C). Advancing and faster completion of flowering and inflorescence growth in isoprene-emitting lines was more pronounced under the high-light regime (Fig. 1F).

Non-emitting controls continued to grow at later stages (>48 DAG) and both ISPS-B2 and C4 lines had significantly lower body mass at the end of 76 DAG compared to non-emitting controls (Fig. S1C). The early-emerging leaves (positions 7 to 12 from the rosette base excluding cotyledons) were significantly bigger in the isoprene-emitting lines than in non-emitting controls. In contrast, the late-emerging leaves (towards the rosette apex) were bigger in control lines than in isoprene-emitting lines (Fig. S1D).

Poplar: Apical growth rate in isoprene-emitting (WT and EV) lines was significantly greater than the RANi isoprene-suppressed (RA1 and RA2) lines during summer (July-September 2018), but the difference became less prominent during early-autumn (October 2018, Fig. 2A). The difference in apical growth rate was most pronounced during mid-summer (July 1 to Aug 15), when the average day temperature was 36 ± 2 °C between 11 am and 4 pm (Fig. 2A). When averaged for the whole growing season the apical growth rate remained significantly higher in isoprene-emitting lines. These trends were conserved during the following summer. The leaf area of isoprene-emitting poplars was bigger than in RA1 and RA2 only in some leaves emerging in mid-summer (Fig. 2B), whereas all other leaves showed similar phenotypes. Bigger leaves of isoprene-emitting poplar lines showed significantly lower fresh weight to dry weight ratio (4.4 ± 0.18), hence lower tissue density compared to isoprene-suppressed lines (4.1 ± 0.09). The isoprene-suppressed poplars showed a distinct plant architecture at the end of the growing season, with lower apical stems, longer lower branches and a bushier appearance compared to isoprene-emitting controls (Fig. 2C).

Photosynthesis and leaf energy status

Arabidopsis: Isoprene-emitting ISPS-B2 and ISPS-C4 *Arabidopsis* lines showed lower P_n compared to non-emitting controls under low-light regime (Fig. 3A; measured only on fully expanded leaves before and after flowering). However, electron transport rate and stomatal conductance were not different in isoprene-emitting and non-emitting lines (Fig. S2A, S2B, S2C). All lines showed equivalent

photosynthetic rates under high-light except ISPS-C4 leaves that showed the highest P_n at 28 DAG (before flowering). After flowering, P_n declined significantly in all lines. The decline was steeper and more significant in isoprene-emitting lines in both low-light and high-light regimes (Fig. 3A, 3B). Chlorophyll fluorescence maximal quantum yield decreased significantly more in older (76 DAG) rosette leaves of the isoprene-emitting ISPS-C4 line (Fig. 3C).

Poplar: Net photosynthetic rate of summer leaves was not significantly different among lines at 30 and 60 DAE (Fig. 4A). Both spring- and summer-emerging leaves of RA1 and RA2 isoprene-suppressed lines showed a significantly higher P_n than WT and EV isoprene-emitting leaves at older leaf age ($\geq$90 DAE, Fig. 4A, S3). V_{cmax} was higher in non-emitting RA1 summer leaves at 60 DAE and it remained significantly higher in older ($\geq$90 DAE) leaves of both RA1 and RA2 (Fig. 4B).

Measurements of chlorophyll fluorescence further showed that age-dependent decline of photosynthetic electron transport rate (ETR) and maximum quantum yield of photosystem II occurred earlier in isoprene-emitting than in non-emitting leaves ($\geq$90 DAE, Fig. 4C, 4D). Emitting and non-emitting leaves showed no significant difference in their maximum carboxylation rate by Rubisco (V_{cmax}) when young (30 DAE). Photorespiration rate was significantly greater in RA1 and RA2 summer leaves at 30 and 60 DAE compared to isoprene-emitting controls (Fig. 5A), although the difference became less prominent in older leaves. While there was no difference in ETR among healthy emitting and non-emitting poplar leaves (< 60 DAE; not shown), the relative strength of energy sinks differed significantly among poplar leaves. The proportion of electrons allocated to photosynthetic carbon reduction (J_c) was comparable in isoprene-emitting and non-emitting lines (Fig. 5C) while those allocated to oxygenation (J_o) was significantly higher in non-emitting younger leaves (30 and 60 DAE; Fig. 5D). In contrast, J_c in older isoprene-emitting leaves (> 90 DAE) was significantly lower than that in non-emitting leaves, which corresponded to declining V_{cmax} (Fig. 4B, S3), and increasing ratio of oxygenation to carboxylation by Rubisco in older emitting leaves (120 DAE; Fig. 5B).

Isoprene emission and cytokinin abundance

Arabidopsis: Isoprene-emitting ISPS-C4 *Arabidopsis* line emitted isoprene at a higher rate than ISPS-B2 line. No isoprene was detected from non-emitting controls (Fig. 6A). Isoprene-emitting *Arabidopsis* (sampled at 36 DAG and 48 DAG) showed significantly greater abundance of iPR (isopentenyladenine riboside) and iP (isopentenyladenine) compared to non-emitting lines (Fig. 6 B-E). Even tZR (Fig. S5A, S5B) and cZR (Fig. S5E, S5F) were enriched in isoprene-emitting *Arabidopsis* than in non-emitting lines under low-light regime (not in high-light regime). In *Arabidopsis*, the total CK-riboside level was higher in ISPS-C4, which emitted isoprene at a higher rate, showed faster growth, flowered earliest, and completed lifecycle sooner than the other isoprene-emitting line ISPS-B2.

Poplar: Both WT and EV summer leaves emitted >50 nmol isoprene m^{-2} s^{-1}, while RA1 and RA2 leaves emitted very little (but detectable) amount of isoprene (Fig. 7A). Mature WT and EV poplar leaves (60 DAE) showed significantly greater abundance of iPR and iP (7B, 7C). Abundance of tZR was not always associated with higher levels of active tZ, although abundance of tZOG was proportional to tZ and higher in isoprene emitting-leaves (Fig. 7D, 7E).

Differential gene expression inferred from RNA-seq

Arabidopsis: Isoprene-emitting leaves (line ISPS-C4) showed differential expression of 60 genes under low-light, and 684 genes ($\log_2$[fold change] > [+1.5, <–1.5]; p_{adj}<0.001) under high-light acclimation compared to non-emitting leaves (line EV-B3) of the corresponding light-acclimation group (Fig. 8). Cytokinin oxidase/dehydrogenase were overexpressed in high-light acclimated isoprene-emitting leaves (Fig. 8; Gene IDs: AT2G41510, *CKX1*; AT3G63440, *CKX6*; $\log_2$[foldchange] > 1.5; p_{adj}=0.008 and <0.0001 respectively). Genes coding for chloroplast-specific SIGMA factors and those indicating plastid division were upregulated in isoprene-emitting *Arabidopsis* both under low-light and high-light. Several senescence-associated NAC transcription factors were greater in abundance in isoprene-emitting leaves under low-light and more significantly under high-light regimes. Transcripts coding for *Arabidopsis CONSTANS-like 9* (*COL9*; Gene ID: AT3G07650.1, Seq. ID: NM_001125127.2, $\log_2$[fold change] <–4.7; p_{adj}<0.0001) and *EARLY FLOWERING4* (*ELF4*; Gene ID: AT2G40080, Seq. ID:

NM_129566.2; $\log_2$[fold change] <–2.9, p_{adj}<0.0001)), were significantly depleted in isoprene-emitting *Arabidopsis* leaves (high-light regime, Fig. 8).

Poplar: Suppression of isoprene emission in poplar (line RA1) caused highly significant change (p_{adj}<0.001) in the expression level of 1430 genes in mature fully-expanded leaves (60 DAE) and 5392 genes in older senescing leaves (90 DAE), relative to isoprene-emitting leaves (line WT) of same age. The most prominent $\log_2$[fold change] > [+1.5, <–1.5] was observed for 266 genes at 60 DAE, and 934 genes at 90 DAE. Genes involved in cytokinin metabolism viz. *LOG1 and LOG3* (*LONELEY GUY* family) both coding for cytokinin riboside 5′-monophosphate phosphoribohydrolase that converts inactive CKs to active free bases, and two genes coding for CK oxidase/dehydrogenase (*CKX5* and *CKX7*) that breaks down CKs were significantly down-regulated in isoprene-suppressed RA1 at 60 DAE ($\log_2$[foldchange] < –1.5; p_{adj}<0.00001). Poplar SIGMA factors were downregulated in isoprene-suppressed leaves (60 DAE, Fig. 9). Poplar orthologs of *Arabidopsis COL9* and *ELF3* were enriched in isoprene-suppressed leaves (*ELF3*, $\log_2$[fold change] =3.5; and *COL9*, $\log_2$[fold change] = 2.3; p_{adj}<<0.0001, Fig. 9). Transcripts from heat shock proteins (33 genes coding for various HSP20, HSP70 and HSP90 class proteins) were without exception significantly fewer in isoprene-suppressed poplar leaves. Abundance of many transcripts declined significantly in early-senescing isoprene-emitting WT leaves at 90 DAE, while non-emitting RA1 leaves at 90 DAE remained comparable to their younger versions at 60 DAE. Pairwise comparison between summer WT leaves sampled at 60 DAE and 90 DAE (marking their senescence course), showed that NAC transcription factors (senescence-associated) were significantly upregulated (Fig. S6), while Rubisco-SSU, carbonic anhydrase, and heat shock proteins (HSPs) were downregulated in senescing (90 DAE) isoprene-emitting leaves.

Discussion

Isoprene accelerates plant growth rate, strengthens apical dominance, and induces early leaf and plant senescence

We had hypothesized that isoprene emission may directly affect leaf hormonal status, particularly of isoprenoid-type cytokinins synthesised by the MEP pathway. Significantly high levels of

isopentenyladenine riboside (iPR) and its free base derivative isopentenyladenine (iP) in the leaves of both isoprene-emitting *Arabidopsis* (an annual herb) and poplar (a perennial tree) show that indeed isoprene emission has a direct positive impact on the plastid-localised synthesis of isoprenoid-type CKs via the MEP pathway. We found consistent phenotypic patterns in both model systems, as isoprene-emitting *Arabidopsis* and poplar showed faster growth (Figs. 1A, 1D, 2A), early leaf senescence (Fig. 4A, 5A), and a whole plant phenotype that was distinct from non-emitting lines (Figs. 1B, 1E, 2C). Isoprene has long been shown to stabilise the photosynthetic apparatus under heat and photooxidative stresses (e.g. Sharkey and Singsaas, 1995; Velikova et al. 2011; Pollastri et al. 2019). However, going beyond known physico-mechanical effects of isoprene, we show (in the remaining discussion) a more fundamental and nuanced life-defining role for leaf isoprene emission by its influence on cytokinin synthesis, abundance, hormone-mediated gene regulation, and in shaping plant growth strategies. Our hypothesis and the supporting evidence satisfactorily explain many of the observed metabolic and phenotypic differences between isoprene-emitting and non-emitting plants.

In some ways, it is paradoxical that high CK-riboside abundance led to faster leaf senescence in isoprene-emitting *Arabidopsis* and poplar. A host of two-component signal transduction / response regulators were upregulated in isoprene-emitting leaves (both *Arabidopsis* and poplar, Figs 8, 9), which is consistent with the expected higher activity of CKs. However, we also observed an equivalent and significant overexpression of genes coding for cytokinin oxidase/deoxygenase (*CKX*) in isoprene-emitting leaves (both *Arabidopsis* and poplar, Figs 8, 9). This suggested greater degradation and recycling of isoprenoid-CKs, explained faster development and early senescence in presence of isoprene. Enrichment of transcripts coding for senescence associated NAC transcription factors in both *Arabidopsis* and poplar was also consistent with their early-senescence phenotypes.

Greater apical growth rate and less branching in isoprene-emitting poplars (Fig. 2A, 2C) was another distinct phenotypical change, which suggests strengthening of apical dominance (especially during the early phases of growth) in presence of isoprene, potentially driven by a shift in auxin to CK ratio and hormonal signal transduction throughout the plant body. As iPR is transported in the phloem from

458 leaves to other plant parts (e.g. Hirose et al. 2008), it is possible that excess CKs in isoprene-emitting
459 leaves is transported from the leaves to all meristems, leading to greater CK activity and faster tissue
460 differentiation and expansion. This gives the early growth advantage (and stronger apical dominance)
461 to isoprene-emitting plants described above. The *LOG* genes, coding for CK-riboside monophosphate
462 phosphoribohydrolases involved in activation of CKs and regulation of shoot apical meristematic
463 growth (Kurakawa et al. 2007; Kuroha et al. 2009), were significantly overexpressed in apically
464 dominant isoprene-emitting WT poplars (60 DAE, Fig. 9). Thus, isoprene emission or its absence in
465 leaves appears to affect CK availability throughout the plant body and one of the consequences is likely
466 an altered ratio between auxin and CKs in apical meristems. A recent study reported comparable total
467 biomass accumulation in field-grown (older) isoprene-emitting and suppressed poplar trees (Monson et
468 al. 2020). While we observed a different within plant distribution of biomass (stem to branch ratio) in
469 isoprene-emitting and non-emitting lines, the total biomass among poplar lines was comparable even in
470 our study.
471
472 Isoprene emission also enhanced the abundance of leaf tZR (trans-zeatin riboside, Fig. S4A) which is
473 synthesized mostly in the roots and transported via xylem sap to shoots and leaves (Sakakibara 2006),
474 and also the less active cZR (cis-zeatin riboside, Fig. S4E) originating mostly in the cytosol via
475 prenylation of select tRNAs (Schäfer et al. 2015). High abundance of tZR (*Arabidopsis*) and tZOG
476 (poplar) in isoprene-emitting leaves (synthesised mostly in the roots and also via the foliar MEP
477 pathway; Kasahara et al. 2004), suggests that (a) translocation of these CK-conjugates from roots to
478 leaves is enhanced in presence of isoprene and/or (b) synthesis of all zeatins is locally upregulated in
479 isoprene-emitting leaves. Bigger and thinner leaves of isoprene-emitting *Arabidopsis* and in some
480 isoprene-emitting poplar leaves (depending on the season of emergence) could be driven by the
481 changing ratio of CK-riboside to CK-free bases since both tZR and tZ are implicated in leaf size
482 determination (Osugi et al. 2017). Knowing which CK-species are active in what tissues, and when
483 during leaf development was beyond the scope of this study. We do not know if substrate outflow from
484 the chloroplast to cytosolic mevalonate pathway played a role in enhancing cZR abundance in presence
485 of isoprene. Since several cytokinin response regulators were differentially expressed in presence of

isoprene in both *Arabidopsis* and poplar, we speculate that active CKs such as iP and tZ behave differently and are discriminated by typical two-component response regulators involved in CK-signal transduction in isoprene-emitting leaves.

Isoprene does not influence photosynthesis in young leaves but reduction of photosynthesis marks early senescence in mature leaves

Net photosynthetic rate (P_n) in isoprene-emitting poplar leaves (<60 DAE) was generally greater than in isoprene-supressed lines, although this was not always significant (Fig. 4A, Fig. S3A). However, leaf position and time of emergence (i.e. the age of leaves when they experienced the hottest period of summer) had an impact on how P_n of individual leaves responded to seasonal changes in temperature and when they underwent senescence (Fig. 4A, Fig. S3A). As there was no difference in maximum photochemical yield of PSII and instantaneous photosynthetic electron transport rate among poplar lines (at <60 DAE), isoprene emission likely has limited impact on light reactions of photosynthesis at least in young healthy leaves. As in poplars, electron transport rate and the effective quantum yield of photosystem II in isoprene-emitting lines was equal to that of non-emitting *Arabidopsis* (Fig. S1A) and presumably photosynthesis during early-development (not measurable due to the tiny size of leaves) was similar among all *Arabidopsis* lines under low-light. It is likely that faster expansion of isoprene-emitting *Arabidopsis* leaves might have increased their specific leaf area (thin and less heavy) contributing to lower P_n under low-light (Fig. 3A). However, isoprene-emitting ISPS-C4 *Arabidopsis* showed the highest P_n of all leaves (Fig. 3B), and genes coding for LHCs in photosystems I and II were significantly less suppressed by high-light in ISPS-C4 (Fig. S5), suggesting isoprene-mediated attenuation of high-light suppression of light reactions of photosynthesis. This effect was not evident in poplars likely because they were acclimated to full sun light and hot weather. However, both P_n and F_v/F_m (dark-adapted) declined sooner in older senescing leaves of isoprene-emitting *Arabidopsis* under both low-light and high-light (Figs. 3A-C) and also in older summer-leaves of isoprene emitting poplars (>90 DAE; Figs. 4A, 4C). Both confirming early decline of photosynthesis and faster age-specific downregulation of photosystem II in presence of isoprene. Whilst isoprene-suppression did not always

negatively affect P_n in younger leaves, the abundance of transcripts coding for Rubisco SSU, GAPDH, carbonic anhydrase, and chloroplast RNA-polymerase facilitating SIGMA factors were significantly fewer in isoprene-suppressed poplar leaves compared to emitting leaves (60 DAE, Fig. 9), suggesting overall downregulation of chloroplast metabolism in isoprene-suppressed leaves. In contrast, SIGMA factors and other transcription factors indicative of chloroplast replication were significantly more abundant in isoprene-emitting *Arabidopsis* leaves (Fig. 8), suggesting acceleration of chloroplast division and metabolism in presence of isoprene.

There were significant differences in the relative strengths of energy sinks and their leaf age-specific changes in emitting and non-emitting poplar leaves during leaf senescence (not measured in *Arabidopsis*). Isoprene-suppression was associated with an increased rate of photorespiratory carbon loss at 30 and 60 DAE (Fig. 5A) supporting the broader view that isoprene synthesis (via the MEP pathway) and photorespiration are among several co-localised processes in the chloroplast that maintain the energy source-sink equilibrium while photosynthetic carbon reduction acts as the primary energy sink (Jones and Rasmussen 1975; Dani et al. 2014a). While both carboxylation and oxygenation capacities will be low due to breakdown of Rubisco during senescence in cooler (late-autumn) leaves, oxygenation may take precedence as a means of photoprotection (e.g. Kozaki and Takeba, 1996; Heber et al. 1996) in older senescing leaves where low C_i may favour more photorespiration. This may partly contribute to comparable photorespiration rate and J_o in older leaves among all lines (Fig. 5A, 5D), while V_{cmax}, J_c decreased and v_o/v_c increased more significantly and sooner in older isoprene-emitting summer leaves compared to non-emitting leaves (Fig. 4B, 5B, 5C).

Isoprene induces stress and defense response genes with limited benefits under stress-free conditions

Our poplars were grown under typical Mediterranean summer temperatures (daily max. > 35 °C). Differential expression of a large group of WRKY factors and ethylene response factors (Figs. S7) involved in abiotic stress responses and a sweeping downregulation of many genes coding for heat shock proteins (HSPs) in isoprene-suppressed poplar leaves (60 DAE), show that isoprene emission directly affects stress-response pathways, and this finding broadly agrees with past empirical proofs

showing greater tolerance of isoprene-emitting poplars to intermittent heat (e.g. Behnke et al. 2007), ozone (e.g. Loreto and Velikova 2001) and drought stresses (unpublished). However, the visible downregulation of stress response pathways in RNAi poplars had limited physiological consequence in the study period, which suggested that the conditions were not extreme even for non-emitting poplars. *Arabidopsis* HSPs were reported to be activated during exogenous fumigation with isoprene (Harvey and Sharkey, 2016), but not in our experiments with *Arabidopsis* that made and emitted endogenous isoprene. It is unlikely that isoprene played a thermo and photoprotective role in *Arabidopsis* that were grown at optimal temperature (18 ± 2 °C) and under low light. However, we do not rule out a role for isoprene in priming stress-inducible defense pathways also in *Arabidopsis*. Strikingly, ISPS-C4 also showed the highest isoprene emission rate and CK-riboside levels under both low-light and high-light regimes (Fig. 6A, 6B). We propose that the general stimulation of isoprene emission by transient abiotic stresses (e.g. Sharkey and Loreto 1993; Loreto et al. 2006), likely prevents stress-induced premature leaf senescence potentially also by enrichment of isoprenoid-type CKs in presence of isoprene. While CKs themselves can impart photoprotective benefits (Cortleven and Schmülling, 2015), it is notable that stress induced leaf senescence is characterised by a drop in endogenous CK levels (Pospíšilová et al. 2000) and CK-overexpressing plants can accumulate CK-conjugates, which not only help keep leaves green but also induce photorespiration to prevent photoinhibition under drought (Rivero et al. 2007; 2009). Since isoprene-suppressed young leaves (30 to 60 DAE) had an inherently higher photorespiration potential (despite being CK-poor), isoprene-led CK enrichment is expected to be beneficial in older senescing leaves under stressful conditions. However, faster early growth advantage in isoprene-emitting perennials like poplar can also lead to acute transpiration demand and low stomatal conductance under severe heat and drought (pers. Obs.) and high activity of CKs can negatively impact plant survival under prolonged stresses (Nishiyama et al. 2011). Although not verified in our study, the survival probability of isoprene-emitting poplars is predicted to be lower than non-emitting poplars if the abiotic stress is severe and prolonged (see e.g. Taylor et al. 2018). Therefore, high isoprene emission rate and its positive impact on leaf CK reserves likely become disadvantageous when abiotic stresses become prolonged and severe, unless isoprene synthesis is totally suppressed throughout the stress event (e.g. in resurrection plants, Beckett et al. 2012).

Isoprene induces early flowering, shortens plant generation time, and potentially accelerates diversification of isoprene-emitting lineages

The early flowering in isoprene-emitting *Arabidopsis* lines in both low-light and high-light conditions (Fig. 1C, 1F; also observed by Zuo et al. 2019) is consistent with promotion of flowering by isoprene fumigation in other plants (Terry et al. 1995). It is notable that exogenous CKs (like isoprene) and high endogenous CKs can also promote flowering (Choudhury et al. 1993; Mok, 1994) while CK depletion can delay flowering in annuals (Werner et al. 2003). CK-ribosides and free bases can be enriched when flowering is induced through photoperiodic intervention in annuals (e.g. Bernier et al. 1993; Corbesier et al. 2003). In our experiments, the levels of iPR, iP, and cZR were higher in isoprene-emitting leaves (relative to controls) much before flowering (36 DAG; Fig. S4) and flowering occurred naturally under long-days. Therefore, the high abundance of iPR and cZR in isoprene-emitting leaves sampled before bolting (not observed in non-emitting controls before they flowered relatively later; d.n.s.), supports a role for CKs in inducing early-flowering in presence of isoprene. Overexpression of *CKX* genes in isoprene-emitting leaves and the resulting faster turnover of CKs likely also contributed to advancing of floral induction (e.g. Yang et al. 2003). Significant downregulation of *COL9* and *ELF4,* both negative regulators of flowering time (Covington et al. 2001; Doyle et al. 2002; Cheng and Wang, 2005; Kim et al. 2005), in both isoprene-emitting *Arabidopsis* under high-light may partly account for longer hypocotyls and early flowering in emitting lines (Zuo et al. 2019, also in this study). The *ELF* genes are key regulators of circadian clock and are sensitive to photoperiod also in poplars (Keller et al. 2012) and both *COL9* and *ELF3* were depleted in isoprene-emitting poplar leaves (60 DAE) like in isoprene-emitting *Arabidopsis* (Figs. 8, 9). Faster reproductive maturation and shorter leaf and plant lifespan in isoprene emitting plants are thus linked to potential interaction between isoprene and CK-mediated changes in the circadian and photoperiodic signalling pathways.

Faster growth and early flowering in isoprene-emitting *Arabidopsis* played a role in preventing the expansion of late-emerging isoprene-emitting leaves (positions 16 and above), which remained smaller while those early-emerging leaves were heavier than their counterparts in non-emitting controls (Fig.

S1D). Redistribution of leaf biomass and small apical leaves was partly responsible for low vegetative body mass in emitting lines (particularly ISPS-C4) than non-emitting control lines. Accelerated rate of development in isoprene-emitting *Arabidopsis* not only led to early leaf senescence and early flowering, but also hastened body size maturation and body shrinkage during senescence. Since body size maturation can potentially determine when and how whole-plant senescence proceeds in perennial plants (Dani and Kodandaramaiah, 2019), we hypothesise that the early-riser advantage and the apically dominant (light-competitive) phenotype in naturally isoprene-emitting trees can lead to quicker attainment of body size maturity than in non-emitting taxa. As a result, isoprene-emitting perennial species generally may have shorter generation time (as observed in *Arabidopsis*) and shorter life expectancy than slow growing non-emitting species. Isoprene emission capacity is prevalent among speciose deciduous trees bearing short-lived leaves that are shed seasonally (Dani et al. 2014b). The evidence presented shows how isoprene emission had a role in shortening leaf lifespan and potentially also in faster speciation and diversification of emitting taxa.

Conclusion

Isoprene emission in leaves increased cytokinin abundance, accelerated plant growth, and induced early leaf senescence in both poplar and *Arabidopsis*, and in the latter isoprene also induced early flowering and shortened plant lifespan. Faster leaf senescence and shorter lifecycle (shorter lifespan) in isoprene emitting plants suggests that whenever isoprene emission capacity was acquired in a plant lineage, it potentially contributed to their faster growth and diversification by reducing their generation time. As established by numerous experiments, isoprene may impart photosynthetic stability via membrane interactions and antioxidant activity under transient stressful conditions. Our results add credence to a novel primary role for foliar isoprene emission in altering leaf and organismal development and lifespan, potentially via isoprene-led and/or -mediated enrichment of leaf cytokinins (potentially greater activity and recycling of cytokinins) and cytokinin sensitive transcriptional regulation. The presupposition that there are common selection factors governing leaf senescence, organismal lifespan, isoprene emission and CK metabolism in fast-growing plants is empirically supported.

Acknowledgements

KGSD and FL thank Jonathan Gershenzon (MPICE, Jena), Michele Morgante (IGA, Udine), Maurizio Capuana and Marco Michelozzi (IBBR-CNR, Florence), and Camilla Pandolfi (UNIFI, Florence) for their support. MR acknowledges the support of the Max Planck Society. This work was fully supported by the EU Horizon2020 programme via the Marie Curie fellowship to KGSD under the grant Leaf-Of-Life (2016, 746821) to FL.

References

Anders S, Pyl PT, Huber W (2015). HTSeq - a Python framework to work with high-throughput sequencing data. *Bioinformatics* 31, Issue 2, 166-169. doi:10.1093/bioinformatics/btu638

Behnke, K., Ehlting, B., Teuber, M., Bauerfeind, M., Louis, S., Hänsch, R., ... & Schnitzler, J. P. (2007). Transgenic, non-isoprene emitting poplars don't like it hot. The Plant Journal, 51, 485-499.

Behnke, K., Loivamäki, M., Zimmer, I., Rennenberg, H., Schnitzler, J. P., & Louis, S. (2010). Isoprene emission protects photosynthesis in sunfleck exposed Grey poplar. Photosynthesis Research, 104, 5-17.

Bernier, G., Havelange, A., Houssa, C., Petitjean, A., & Lejeune, P. (1993). Physiological signals that induce flowering. The Plant Cell, 5, 1147-1155.

Chaudhury, A. M., Letham, S., Craig, S., & Dennis, E. S. (1993). amp1-a mutant with high cytokinin levels and altered embryonic pattern, faster vegetative growth, constitutive photomorphogenesis and precocious flowering. The Plant Journal, 4, 907-916.

Cinege, G., Louis, S., Hänsch, R., & Schnitzler, J. P. (2009). Regulation of isoprene synthase promoter by environmental and internal factors. Plant Molecular Biology, 69, 593-604.

Corbesier, L., Prinsen, E., Jacqmard, A., Lejeune, P., Van Onckelen, H., Périlleux, C., & Bernier, G. (2003). Cytokinin levels in leaves, leaf exudate and shoot apical meristem of Arabidopsis thaliana during floral transition. Journal of Experimental Botany, 54, 2511-2517.

Cortleven, A., & Schmülling, T. (2015). Regulation of chloroplast development and function by cytokinin. Journal of Experimental Botany, 66, 4999-5013.

652 Covington, M. F., Panda, S., Liu, X. L., Strayer, C. A., Wagner, D. R., & Kay, S. A. (2001). ELF3
653 modulates resetting of the circadian clock in Arabidopsis. The Plant Cell, 13, 1305-1316.
654 Cheng, X. F., & Wang, Z. Y. (2005). Overexpression of *COL9*, a CONSTANS-LIKE gene, delays
655 flowering by reducing expression of *CO* and *FT* in *Arabidopsis thaliana*. The Plant Journal, 43,
656 758-768.
657 Doyle, M. R., Davis, S. J., Bastow, R. M., McWatters, H. G., Kozma-Bognár, L., Nagy, F., ... &
658 Amasino, R. M. (2002). The ELF4 gene controls circadian rhythms and flowering time in
659 Arabidopsis thaliana. *Nature*, 419, 74-77.
660 Dani, K.G.S., Jamie, I.M., Prentice, I.C. & Atwell, B.J., (2014a). Increased ratio of electron transport
661 to net assimilation rate supports elevated isoprenoid emission rate in eucalypts under drought. Plant
662 Physiology, 166, 1059-1072.
663 Dani, K.G.S., Jamie, I. M., Prentice, I. C., & Atwell, B. J. (2014b). Evolution of isoprene emission
664 capacity in plants. Trends in Plant Science, 19, 439-446.
665 Dani, K.G.S., Fineschi, S., & Loreto, F (2015a). Biogenic volatile isoprenoid emission and levels of
666 natural selection. Journal of the Indian Institute of Science, 95, 1-14.
667 Dani, K.G.S., Jamie, I.M., Prentice, I.C., & Atwell, B.J. (2015b). Species-specific photorespiratory rate,
668 drought tolerance and isoprene emission rate in plants. Plant Signaling & Behavior, 10, e990830.
669 Dani, K.G.S., Fineschi, S., Michelozzi, M., & Loreto, F. (2016). Do cytokinins, volatile isoprenoids
670 and carotenoids syngergically delay leaf senescence? Plant, Cell and Environment 39, 1103-1111.
671 Dani, K.G.S., Kodandaramaiah, U. (2019) Ageing in trees, Role of body size optimization in
672 demographic senescence, Perspectives in Plant Ecology, Evolution, and Systematics, 36, (page
673 number yet to be assigned, in press).
674 Del Fabbro C, Scalabrin S, Morgante M, Giorgi FM (2013). An Extensive Evaluation of Read
675 Trimming Effects on Illumina NGS Data Analysis. PLoS One 8, e85024.
676 https://doi.org/10.1371/journal.pone.0085024
677 Dobin A, Davis CA, Schlesinger F, Drenkow J, Zaleski C, Jha S, Batut P, Chaisson M, Gingeras TR
678 (2013). STAR: Ultrafast universal RNA-seq aligner. Bioinformatics 29, 15–21.

679 Guenther, A., Karl, T., Harley, P., Wiedinmyer, C., Palmer, P. I., & Geron, C. (2006). Estimates of
680 global terrestrial isoprene emissions using MEGAN (Model of Emissions of Gases and Aerosols
681 from Nature). Atmospheric Chemistry and Physics, 6, 3181-3210.
682 Guo, Y., & Gan, S. S. (2014). Translational researches on leaf senescence for enhancing plant
683 productivity and quality. Journal of Experimental Botany, 65, 3901-3913.
684 Harvey, C. M., & Sharkey, T. D. (2016). Exogenous isoprene modulates gene expression in unstressed
685 *Arabidopsis* thaliana plants. Plant, Cell & Environment, 39, 1251-1263.
686 Heber, U., Bligny, R., Streb, P., & Douce, R. (1996). Photorespiration is essential for the protection of
687 the photosynthetic apparatus of C3 plants against photoinactivation under sunlight. Plant Biology,
688 109: 307-315.
689 Hirose, N., Takei, K., Kuroha, T., Kamada-Nobusada, T., Hayashi, H., & Sakakibara, H. (2007).
690 Regulation of cytokinin biosynthesis, compartmentalization and translocation. Journal of
691 Experimental Botany, 59, 75-83.
692 Kasahara, H., Takei, K., Ueda, N., Hishiyama, S., Yamaya, T., Kamiya, Y., ... & Sakakibara, H. (2004).
693 Distinct isoprenoid origins of cis-and trans-zeatin biosyntheses in *Arabidopsis*. Journal of
694 Biological Chemistry, 279, 14049-14054.
695 Keller, S. R., Levsen, N., Olson, M. S., & Tiffin, P. (2012). Local adaptation in the flowering-time gene
696 network of balsam poplar, Populus balsamifera L. Molecular Biology and Evolution, 29, 3143-
697 3152.
698 Kim, W. Y., Hicks, K. A., & Somers, D. E. (2005). Independent roles for *EARLY FLOWERING 3* and
699 *ZEITLUPE* in the control of circadian timing, hypocotyl length, and flowering time. Plant
700 Physiology, 139, 1557-1569.
701 Kozaki, A., & Takeba, G. (1996). Photorespiration protects C3 plants from photooxidation. Nature,
702 384, 557-560.
703 Kurakawa, T., Ueda, N., Maekawa, M., Kobayashi, K., Kojima, M., Nagato, Y., ... & Kyozuka, J.
704 (2007). Direct control of shoot meristem activity by a cytokinin-activating enzyme. *Nature*, 445,
705 652-655.

706 Kuroha, T., Tokunaga, H., Kojima, M., Ueda, N., Ishida, T., Nagawa, S., ... & Sakakibara, H. (2009).
707 Functional analyses of LONELY GUY cytokinin-activating enzymes reveal the importance of the
708 direct activation pathway in Arabidopsis. *The Plant Cell*, 21, 3152-3169.
709 Li, M., Xu, J., Algarra Alarcon, A., Carlin, S., Barbaro, E., Cappellin, L., ... & Varotto, C. (2017). In
710 planta recapitulation of isoprene synthase evolution from Ocimene synthases. Molecular Biology
711 and Evolution, 34, 2583-2599.
712 Li, Z & Sharkey, T.D. (2013) Metabolic profiling of the methylerythritol phosphate pathway reveals
713 the source of post-illumination isoprene burst from leaves, Plant Cell & Environment. 36, 429-
714 437.
715 Loivamäki, M., Gilmer, F., Fischbach, R. J., Sörgel, C., Bachl, A., Walter, A., & Schnitzler, J. P. (2007).
716 Arabidopsis, a model to study biological functions of isoprene emission? Plant Physiology, 144,
717 1066-1078.
718 Loreto, F., & Schnitzler, J. P. (2010). Abiotic stresses and induced BVOCs. Trends in Plant Science, 15,
719 154-166.
720 Loreto, F., Bagnoli, F., Calfapietra, C., Cafasso, D., De Lillis, M., Filibeck, G., ... & Ricotta, C. (2014).
721 Isoprenoid emission in hygrophyte and xerophyte E uropean woody flora, ecological and
722 evolutionary implications. Global Ecology and Biogeography, 23, 334-345.
723 Loreto, F., Mannozzi, M., Maris, C., Nascetti, P., Ferranti, F., & Pasqualini, S. (2001). Ozone quenching
724 properties of isoprene and its antioxidant role in leaves. Plant Physiology, 126, 993-1000.
725 Love MI, Huber W and Anders S (2014). Moderated estimation of fold change and dispersion for RNA-
726 seq data with DESeq2. Genome Biology, 15, pp. 550. doi: 10.1186/s13059-014-0550-8.
727 Martin M (2011). Cutadapt removes adapter sequences from high-throughput sequencing reads.
728 EMBnet.journal, 17 10-12.
729 McFiggans, G., Mentel, T. F., Wildt, J., Pullinen, I., Kang, S., Kleist, E., ... & Zhao, D. (2019).
730 Secondary organic aerosol reduced by mixture of atmospheric vapours. *Nature*, 565, 587-593.
731 Mok, M. C. (1994). Cytokinins and plant development. In, *Cytokinins, Chemistry, Activity and*
732 *Function*, (Eds, Mok D.W.S. & Mok, M.C.) CRC Press, Inc, Florida, USA, pp 155-166

733 Monson, R. K., Jones, R. T., Rosenstiel, T. N., & Schnitzler, J. P. (2013). Why only some plants emit
734 isoprene? *Plant, Cell & Environment*, 36, 503-516.
735 Mutanda, I., Inafuku, M., Saitoh, S., Iwasaki, H., Fukuta, M., Watanabe, K., & Oku, H. (2016).
736 Temperature controls on the basal emission rate of isoprene in a tropical tree *Ficus septica*,
737 exploring molecular regulatory mechanisms. Plant, Cell & Environment, 39, 2260-2275.
738 Nishiyama, R., Watanabe, Y., Fujita, Y., Le, D. T., Kojima, M., Werner, T.… & Sakakibara, H. (2011).
739 Analysis of cytokinin mutants and regulation of cytokinin metabolic genes reveals important
740 regulatory roles of cytokinins in drought, salt and abscisic acid responses, and abscisic acid
741 biosynthesis. The Plant Cell, 23, 2169-2183.
742 Osugi, A., Kojima, M., Takebayashi, Y., Ueda, N., Kiba, T., & Sakakibara, H. (2017). Systemic
743 transport of trans-zeatin and its precursor have differing roles in *Arabidopsis* shoots. Nature Plants,
744 3, 17112.
745 Peñuelas, J., & Munné-Bosch, S. (2005). Isoprenoids, an evolutionary pool for photoprotection. Trends
746 in Plant Science, 10, 166-169.
747 Pollastri, S., Tsonev, T., & Loreto, F. (2014). Isoprene improves photochemical efficiency and enhances
748 heat dissipation in plants at physiological temperatures. Journal of Experimental Botany, 65, 1565-
749 1570.
750 Pospíšilová, J., Synková, H., & Rulcová, J. (2000). Cytokinins and water stress. Biologia Plantarum,
751 43, 321-328.
752 Raines, T., Shanks, C., Cheng, C. Y., McPherson, D., Argueso, C. T., Kim, H. J., ... & Schaller, G. E.
753 (2016). The cytokinin response factors modulate root and shoot growth and promote leaf
754 senescence in *Arabidopsis*. The Plant Journal, 85, 134-147.
755 Rivero, R. M., Kojima, M., Gepstein, A., Sakakibara, H., Mittler, R., Gepstein, S., & Blumwald, E.
756 (2007). Delayed leaf senescence induces extreme drought tolerance in a flowering plant.
757 Proceedings of the National Academy of Sciences, 104, 19631-19636.
758 Rivero, R. M., Shulaev, V., & Blumwald, E. (2009). Cytokinin-dependent photorespiration and the
759 protection of photosynthesis during water deficit. *Plant Physiology*, 150: 1530-1540.

760 Sakakibara, H. (2006). Cytokinins, activity, biosynthesis, and translocation. Annu. Rev. Plant Biol., 57,
761 431-449.
762 Schäfer, M., Brütting, C., Meza-Canales, I. D., Großkinsky, D. K., Vankova, R., Baldwin, I. T., &
763 Meldau, S. (2015). The role of cis-zeatin-type cytokinins in plant growth regulation and mediating
764 responses to environmental interactions. Journal of Experimental Botany, 66, 4873-4884.
765 Schäfer, M., Reichelt, M., Baldwin, I. & Meldau, S. (2014). Cytokinin Analysis, Sample Preparation
766 and Quantification. Bio-protocol 4, e1167.
767 Schnitzler, J. P., Zimmer, I., Bachl, A., Arend, M., Fromm, J., & Fischbach, R. J. (2005). Biochemical
768 properties of isoprene synthase in poplar (*Populus× canescens*). *Planta*, *222*, 777-786.
769 Sharkey, T. D., & Monson, R. K. (2014). The future of isoprene emission from leaves, canopies and
770 landscapes. Plant, Cell & Environment, 37, 1727-1740.
771 Sharkey, T. D., & Singsaas, E. L. (1995). Why plants emit isoprene. Nature, 374, 769-769.
772 Sharkey, T. D., & Yeh, S. (2001). Isoprene emission from plants. Annual Review of Plant Biology, 52,
773 407-436.
774 Terry, G. M., Stokes, N. J., Hewitt, C. N., & Mansfield, T. A. (1995). Exposure to isoprene promotes
775 flowering in plants. Journal of Experimental Botany, 46, 1629-1631.
776 Velikova, V., Brunetti, C., Tattini, M., Doneva, D., Ahrar, M., Tsonev, T., ... & Varotto, C. (2016).
777 Physiological significance of isoprenoids and phenylpropanoids in drought response of
778 Arundinoideae species with contrasting habitats and metabolism. Plant, Cell & Environment, 39,
779 2185-2197.
780 Velikova, V., Várkonyi, Z., Szabó, M., Maslenkova, L., Nogues, I., Kovács, L., ... & Loreto, F. (2011).
781 Increased Thermostability of Thylakoid Membranes in Isoprene-Emitting Leaves Probed with
782 Three Biophysical Techniques. Plant Physiology, 157, 905-916.
783 Vickers, C. E., Possell, M., Cojocariu, C. I., Velikova, V. B., Laothawornkitkul, J., Ryan, A., ...&
784 Nicholas Hewitt, C. (2009). Isoprene synthesis protects transgenic tobacco plants from oxidative
785 stress. Plant, Cell & Environment, 32, 520-531.
786 Werner, T., Motyka, V., Laucou, V., Smets, R., Van Onckelen, H., & Schmülling, T. (2003). Cytokinin-
787 deficient transgenic *Arabidopsis* plants show multiple developmental alterations indicating

opposite functions of cytokinins in the regulation of shoot and root meristem activity. The Plant Cell, 15, 2532-2550.

Werner, T., Motyka, V., Strnad, M., & Schmülling, T. (2001). Regulation of plant growth by cytokinin. Proceedings of the National Academy of Sciences, 98, 10487-10492.

Yang, S., Yu, H., Xu, Y., & Goh, C. J. (2003). Investigation of cytokinin-deficient phenotypes in Arabidopsis by ectopic expression of orchid DSCKX1. FEBS letters, 555, 291-296.

Zavaleta-Mancera, H. A., López-Delgado, H., Loza-Tavera, H., Mora-Herrera, M., Trevilla-García, C., Vargas-Suárez, M., & Ougham, H. (2007). Cytokinin promotes catalase and ascorbate peroxidase activities and preserves the chloroplast integrity during dark-senescence. Journal of Plant Physiology, 164, 1572-1582

Zhang, H., Dugé de Bernonville, T., Body, M., Glevarec, G., Reichelt, M., … Giron, D. (2016). Leaf-mining by *Phyllonorycter blancardella* reprograms the host-leaf transcriptome to modulate phytohormones associated with nutrient mobilization and plant defense. Journal of Insect Physiology, 84, 114-127.

Zuo, Z., Weraduwage, S. M., Lantz, A. T., Sanchez, L. M., Weise, S. E., Wang, J., ... & Sharkey, T. D. (2019). Isoprene acts as a signaling molecule in gene networks important for stress responses and plant growth. Plant Physiology, 180, 124-152.

Figure captions

Figure 1. Growth, vegetative phenotype, and flowering isoprene-emitting and non-emitting *Arabidopsis* acclimated to (A, B, C) low-light intensity (100 µmol photons m^{-2} s^{-1}) and (E, F, G) high-light intensity (200 µmol photons m^{-2} s^{-1}). (A, D) Above ground biomass (sampled at 28 DAG), which was significantly higher in isoprene-emitting lines. (B, E) Photographs showing whole-plant phenotype in WT: Wild Type, EV-B3: Empty Vector control, ISPS-B2 and ISPS-C4: transgenic isoprene emitting lines. ISPS-C4 shows the most distinct phenotype and leaf size distribution under high-light (also see Fig. 2B), (C, F) Early-flowering and faster completion of inflorescence growth in isoprene-emitting lines. The box for each line includes the median (the horizontal line within the box) and the box marks the lower and upper quartiles. The whiskers span the full data range. Means that are significantly different do not share alphabetical letter codes ($N \geq 10$ biological replicates, Tukey's test, α=0.05).

Figure 2: Growth, leaf and plant phenotype in isoprene-emitting and non-emitting poplars (A) sub-seasonal variation in apical growth rate (cm per month), (B) leaf phenotype in spring- and summer-emerging leaves, (C) plant phenotype in 6-month-old (July) and 10-month-old saplings (October). The box for each line includes the mean (a circle with a plus mark), the median (the middle horizontal line) and the box spans lower and upper quartiles. The whiskers span the full data range. ($N \geq 6$ biological replicates, Tukey's test, α=0.05).

Figure 3. Net photosynthetic rate (P_n) in fully mature Arabidopsis leaves (A) 48 and 64 days after germination under low-light intensity and (B) 28 and 48 days after germination under high-light intensity, WT: Wild Type, EV-B3: Empty Vector control, ISPS-B2 and ISPS-C4: transgenic isoprene emitting lines ($N = 6$ individuals each, Tukey's test, α=0.05). Means that are significantly different do not share alphabetical letter codes. (C) Chlorophyll fluorescence images showing the quantum yield of photosystem II (Y(II)) and the extent of leaf senescence in basal rosette leaves of *Arabidopsis* (72 days after germination).

Figure 4: Leaf age-specific changes in photosynthesis in summer-leaves of poplar from leaf maturity to late stages of senescence. (A) Net photosynthetic rate (P_n) and (B) Maximum carboxylation rate by RuBisCO (V_{cmax}) measured in leaves at 30, 60, 90 and 120 days after leaf emergence. (C) Representative chlorophyll fluorescence images showing the quantum yield of photosystem II (Y(II)) and (D) Fv/Fm estimates showing the extent of leaf senescence at 60 and 90 DAE. The box for each line includes the mean and the box spans lower and upper quartiles. The whiskers span the full data range ($N \geq 10$, Tukey's test, α=0.05). Means that are significantly different do not share alphabetical letter codes.

Figure 5: Leaf age-specific changes in chloroplast energy status of summer-leaves of poplar from leaf maturity to late-senescence (A) photorespiration rate, (B) v_o/v_c ratio, (C) electron transport rate invested in photosynthetic carbon reduction (J_c), and (D) electron transport rate available for photorespiration (J_o) measured in leaves at 30, 60, 90 and 120 days after emergence. The box for each line includes the mean and the box spans lower and upper quartiles. The whiskers span the full data range ($N \geq 10$, Tukey's test, α=0.05). Means that are significantly different do not share alphabetical letter codes.

Figure 6. Isoprene emission rate and abundance of cytokinins in *Arabidopsis* leaves (A) Isoprene emission rate measured at 20 °C, low and high-light treatment); (B) and (C) isopentenyladenine riboside (iPR) abundance, (D) and (E) isopentenyladenine (iP) abundance at 36 and 48 days after germination respectively. The box for each line spans the full data range and includes values from 3 to 5 true biological replicates, where each replicate comprised leaves sampled from up to 5 individuals per line (Kruskal-Wallis H test, α=0.05). Medians that are significantly different do not share alphabetical letter codes

Figure 7. Isoprene emission rate and abundance of cytokinins in summer-leaves (60 days after emergence) in poplar (A) Isoprene emission rate measured at 25 °C, 1500 µmol photons m^{-2} s^{-1}; and abundance of cytokinins namely (B) isopentenyladenine riboside, iPR; (C) isopentenyladenine, iP; (D) trans zeatin, tZ; and (E) trans zeatin-o-glucoside. The box for each line spans the full data range and includes the mean and the median ($N \geq 4$ biological replicates, ≥3 leaves pooled per sample per individual; Games-Howell test, α=0.05). Means that are significantly different do not share alphabetical letter codes.

Figure 8. Differential gene expression in transgenic isoprene-emitting *Arabidopsis* compared to non-emitting control. Most significant $\log_2$[fold change] in transcript abundance during pairwise comparison between

low-light and high-light acclimated vector control leaves (EV-B3) and isoprene-emitting leaves (ISPS-C4) are shown. Likewise, pairwise comparison between non-emitting and isoprene-emitting leaves is also shown under low-light and high-light treatment. The gene IDs correspond to the latest annotation of *Arabidopsis thaliana* genome (TAIR10). Darker the blue, more depleted are the transcripts in isoprene-emitting leaves and similarly brighter the red, more enriched are the transcripts in presence of isoprene. Wherever $\log_2$[fold change] is > +1.5 and <−1.5, the corresponding p_{adj} is <0.001. Wherever the fold change is less prominent but significant p_{adj} is often <0.05, and non-significant change is represented by white blanks.

Figure 9. Differential gene expression in transgenic isoprene-suppressed poplar summer leaves compared to isoprene-emitting wild type leaves. Most significant $\log_2$[fold change] in transcript abundance during pairwise comparison between WT isoprene-emitting leaves and RA1 isoprene-suppressed leaves are shown for leaves at 60 and 90 days after emergence (DAE). Darker the blue, more depleted are the transcripts in isoprene-suppressed RA1 leaves while brighter the red, more enriched are the transcripts in RA1 leaves relative to the corresponding isoprene-emitting WT leaves at 60 DAE and 90 DAE. In a third column, changes in gene expression during the natural course of autumn leaf senescence in poplar is represented by a pairwise comparison between WT isoprene-emitting leaves at 90 DAE (relative to WT leaves at 60 DAE). In this third column, brighter red corresponds to the more expression in senescing WT leaves (90 DAE) and darker blue indicate low expression in senescing WT leaves (90 DAE). The gene IDs and chromosomal loci correspond to the latest annotation of *Populus trichocarpa* whole genome available at NCBI. The foldchange statistical interpretation is as in Fig. 8.

Figure 1

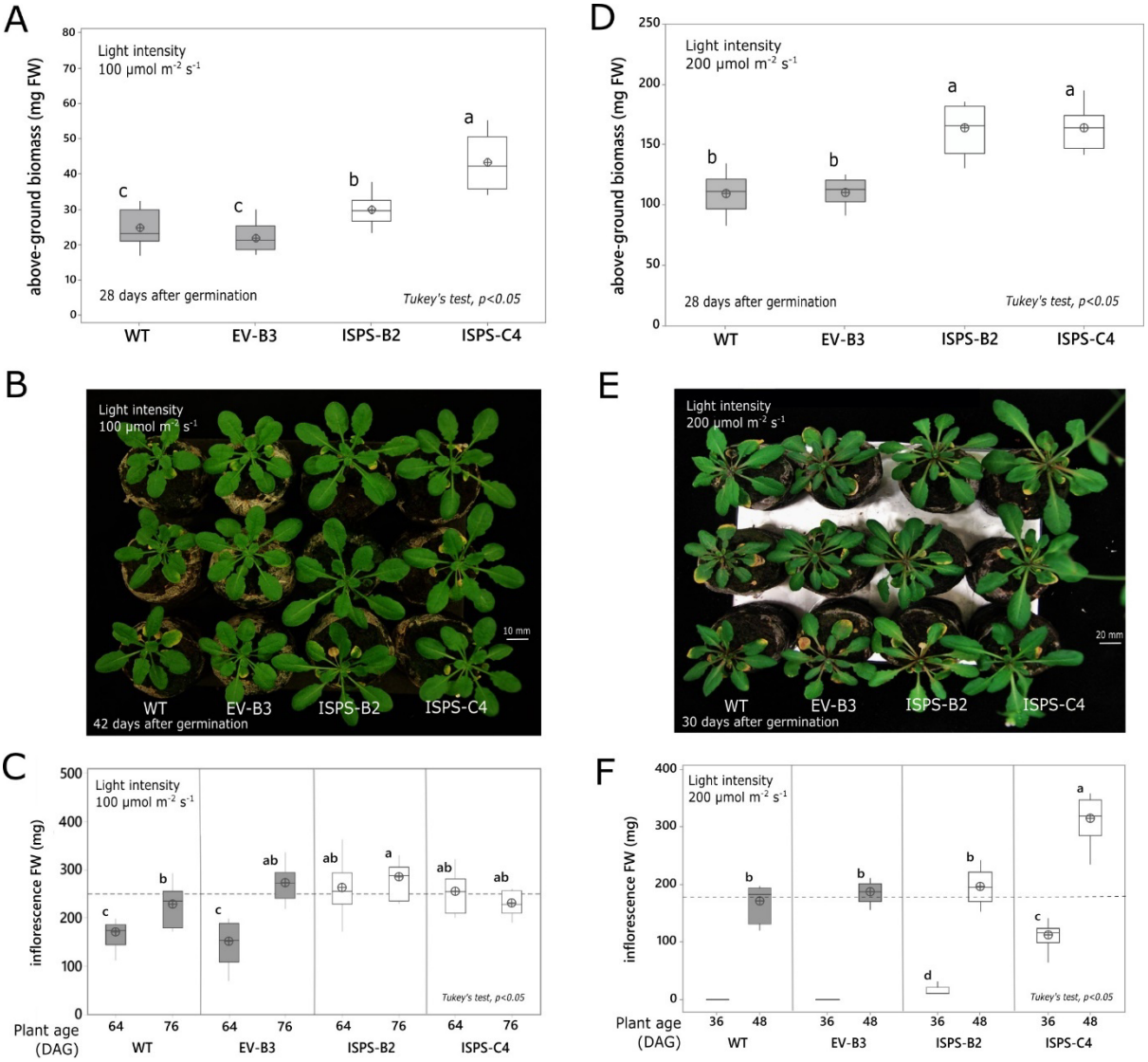
A
Light intensity
100 µmol m-2 s-1
above-ground biomass (mg FW)
28 days after germination
Tukey's test, p<0.05
WT
EV-B3
ISPS-B2
ISPS-C4
D
Light intensity
200 µmol m-2 s-1
above-ground biomass (mg FW)
28 days after germination
Tukey's test, p<0.05
B
Light intensity
100 µmol m-2 s-1
10 mm
42 days after germination
E
Light intensity
200 µmol m-2 s-1
20 mm
30 days after germination
C
Light intensity
100 µmol m-2 s-1
inflorescence FW (mg)
Plant age (DAG)
F
Light intensity
200 µmol m-2 s-1
inflorescence FW (mg)
Plant age (DAG)

Figure 2

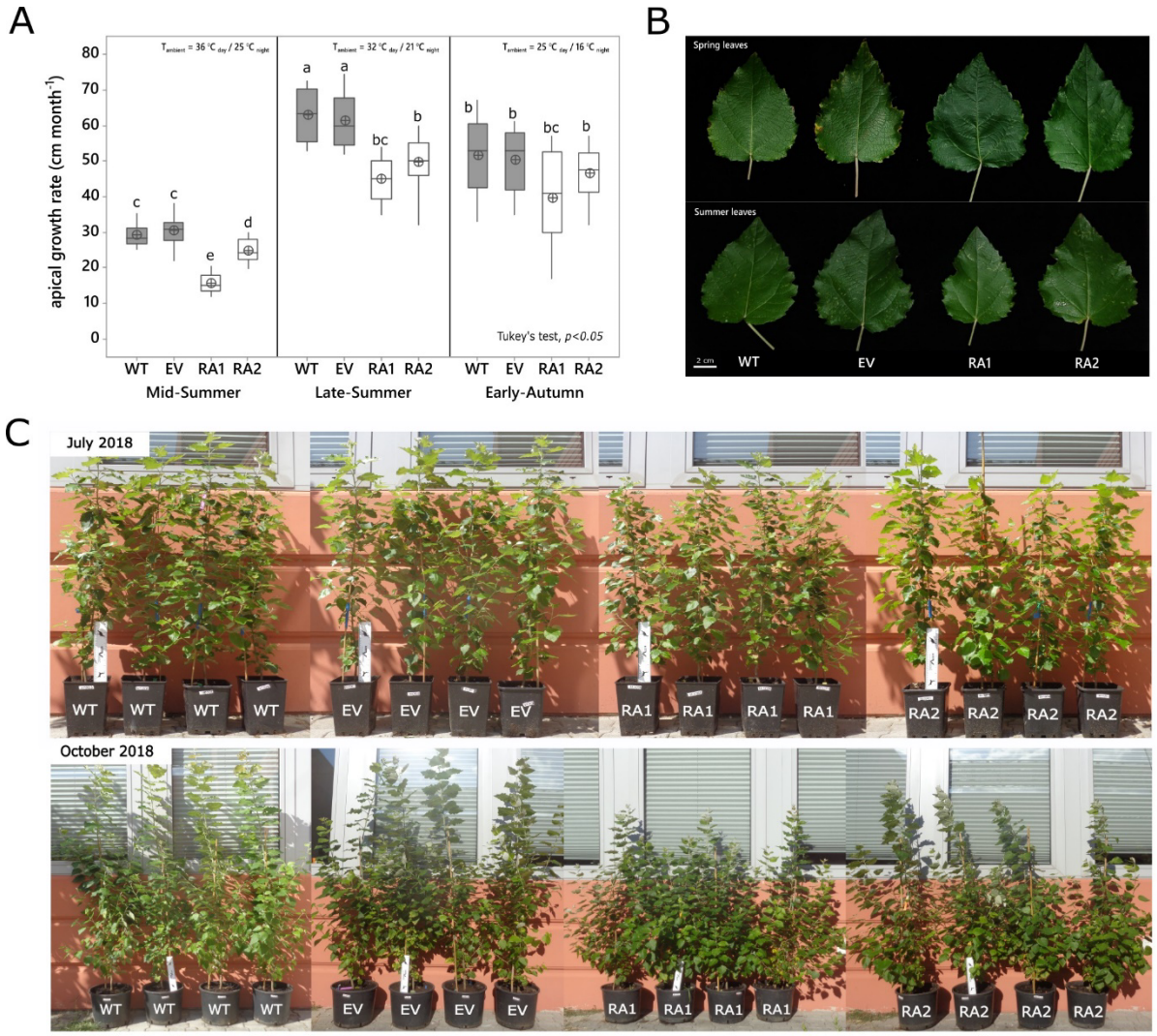
A
B
C
apical growth rate (cm month-1)
Tukey's test, p<0.05
WT EV RA1 RA2
Mid-Summer
Late-Summer
Early-Autumn
Spring leaves
Summer leaves
2 cm
July 2018
October 2018

Figure 3

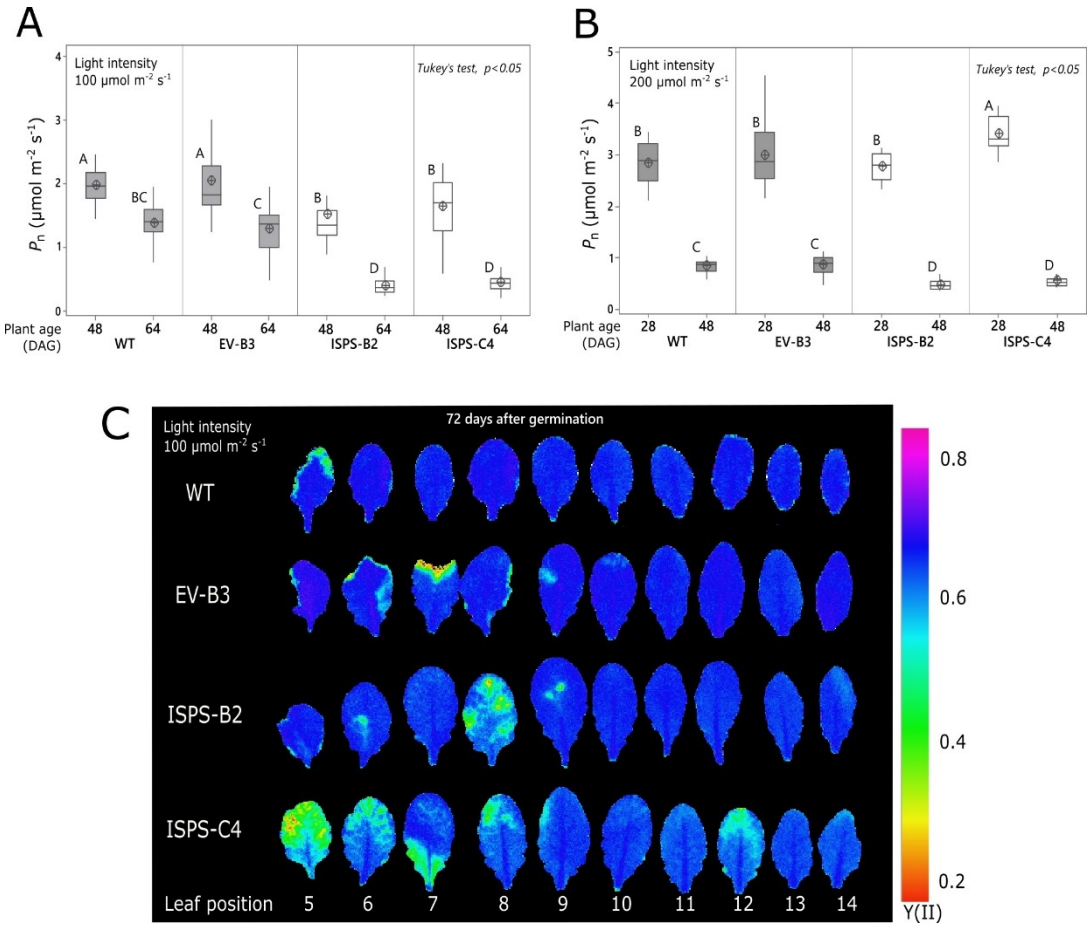
A
Light intensity
100 µmol m-2 s-1
Tukey's test, p<0.05
Pn (µmol m-2 s-1)
Plant age (DAG)
WT
EV-B3
ISPS-B2
ISPS-C4
B
Light intensity
200 µmol m-2 s-1
Tukey's test, p<0.05
C
72 days after germination
Light intensity
100 µmol m-2 s-1
WT
EV-B3
ISPS-B2
ISPS-C4
Leaf position
Y(II)

Figure 4

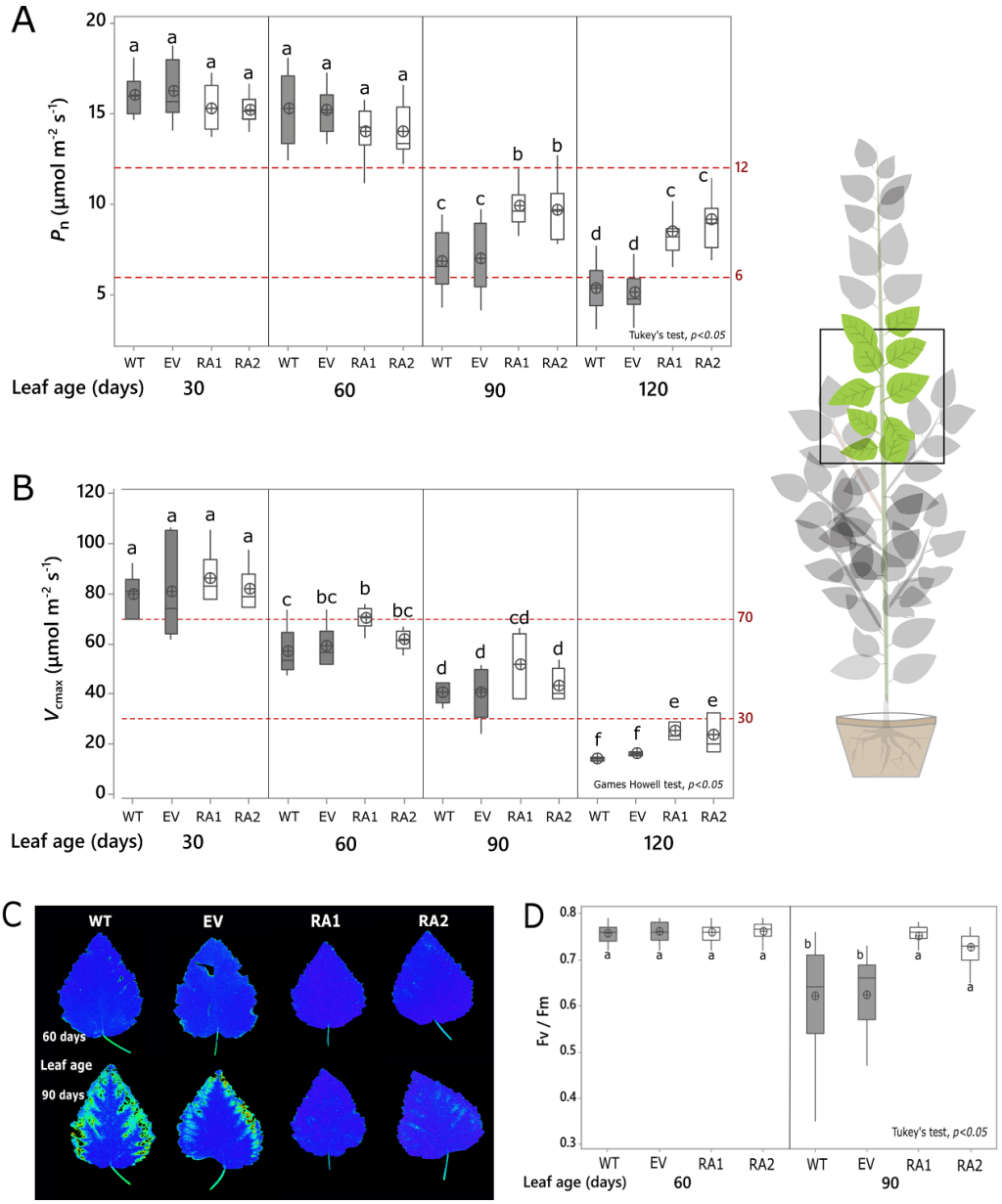
A
P_n (µmol m^{-2} s^{-1})
Tukey's test, p<0.05
B
V_{cmax} (µmol m^{-2} s^{-1})
Games Howell test, p<0.05
WT EV RA1 RA2
Leaf age (days) 30 60 90 120
C
WT EV RA1 RA2
60 days
Leaf age
90 days
D
Fv / Fm
Tukey's test, p<0.05
Leaf age (days) 60 90

Figure 5

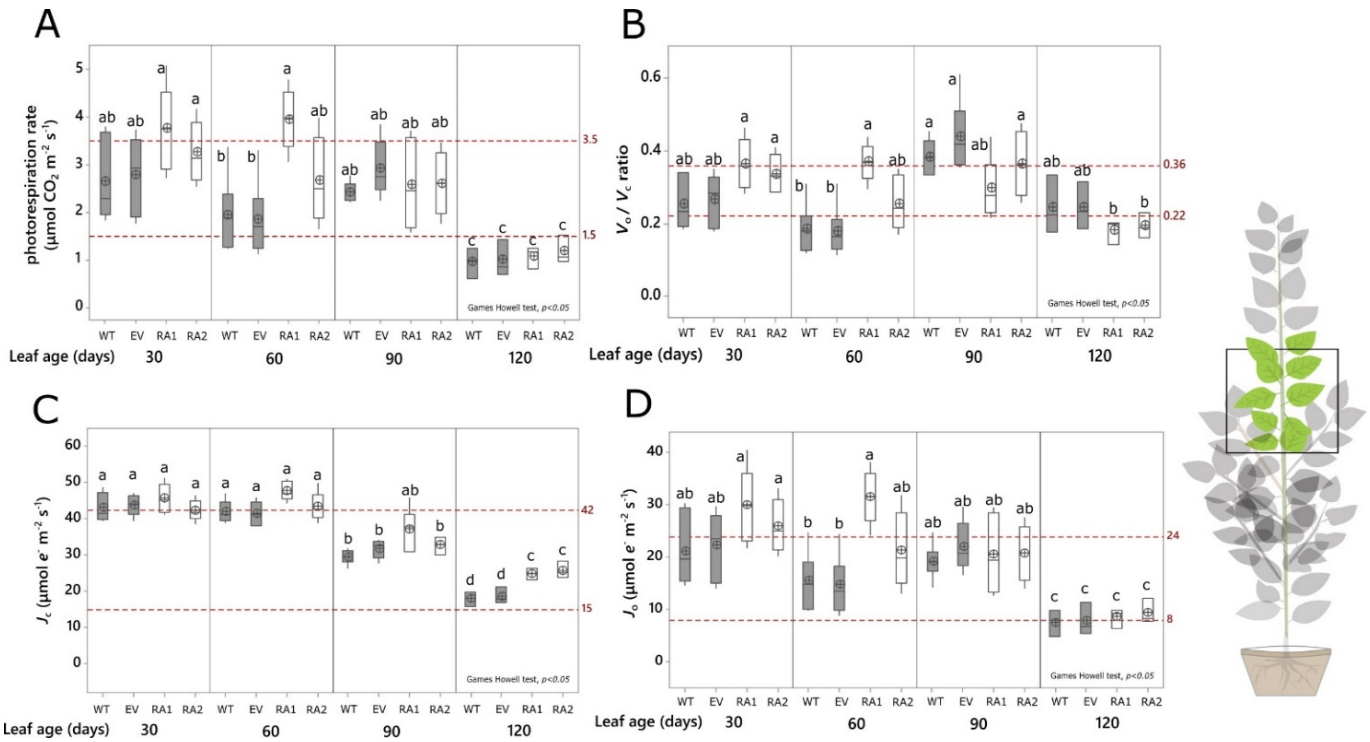
A
photorespiration rate (μmol CO_2 m^{-2} s^{-1})
3.5
1.5
Games Howell test, p<0.05
WT EV RA1 RA2 WT EV RA1 RA2 WT EV RA1 RA2 WT EV RA1 RA2
Leaf age (days) 30 60 90 120
B
V_o / V_c ratio
0.36
0.22
Games Howell test, p<0.05
Leaf age (days) 30 60 90 120
C
J_c (μmol e^- m^{-2} s^{-1})
42
15
Games Howell test, p<0.05
Leaf age (days) 30 60 90 120
D
J_o (μmol e^- m^{-2} s^{-1})
24
8
Games Howell test, p<0.05
Leaf age (days) 30 60 90 120

Figure 6

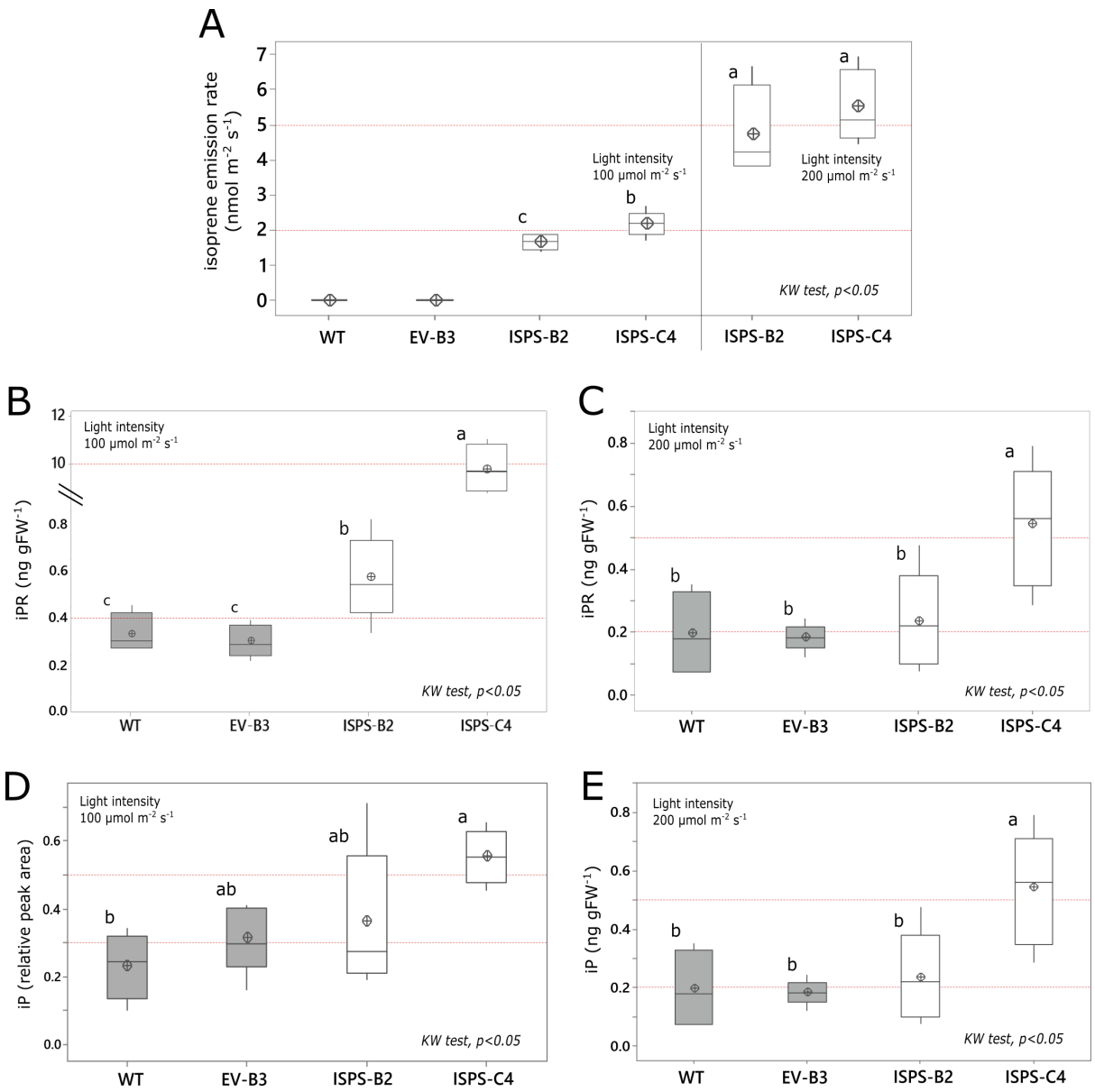
A
isoprene emission rate (nmol m-2 s-1)
Light intensity 100 µmol m-2 s-1
Light intensity 200 µmol m-2 s-1
KW test, p<0.05
WT
EV-B3
ISPS-B2
ISPS-C4
B
iPR (ng gFW-1)
C
D
iP (relative peak area)
E
iP (ng gFW-1)

Figure 7

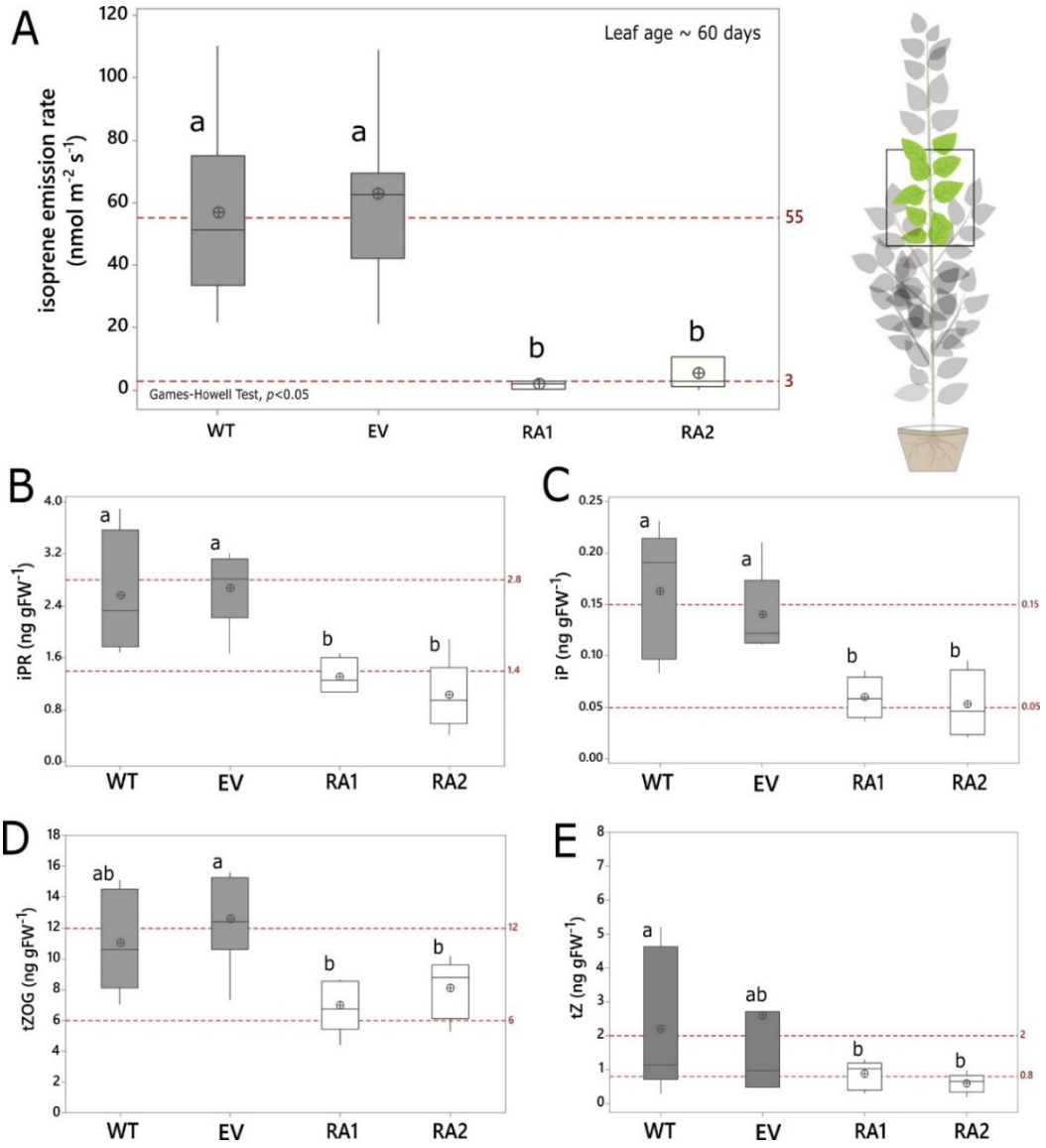
A
Leaf age ~ 60 days
isoprene emission rate (nmol m-2 s-1)
120
100
80
60
40
20
0
a
a
b
b
55
3
Games-Howell Test, p<0.05
WT
EV
RA1
RA2
B
iPR (ng gFW-1)
4.0
3.2
2.4
1.6
0.8
0.0
a
a
b
b
2.8
1.4
WT
EV
RA1
RA2
C
iP (ng gFW-1)
0.25
0.20
0.15
0.10
0.05
0.00
a
a
b
b
0.15
0.05
WT
EV
RA1
RA2
D
tZOG (ng gFW-1)
18
16
14
12
10
8
6
4
2
0
ab
a
b
b
12
6
WT
EV
RA1
RA2
E
tZ (ng gFW-1)
8
7
6
5
4
3
2
1
0
a
ab
b
b
2
0.8
WT
EV
RA1
RA2

Figure 8

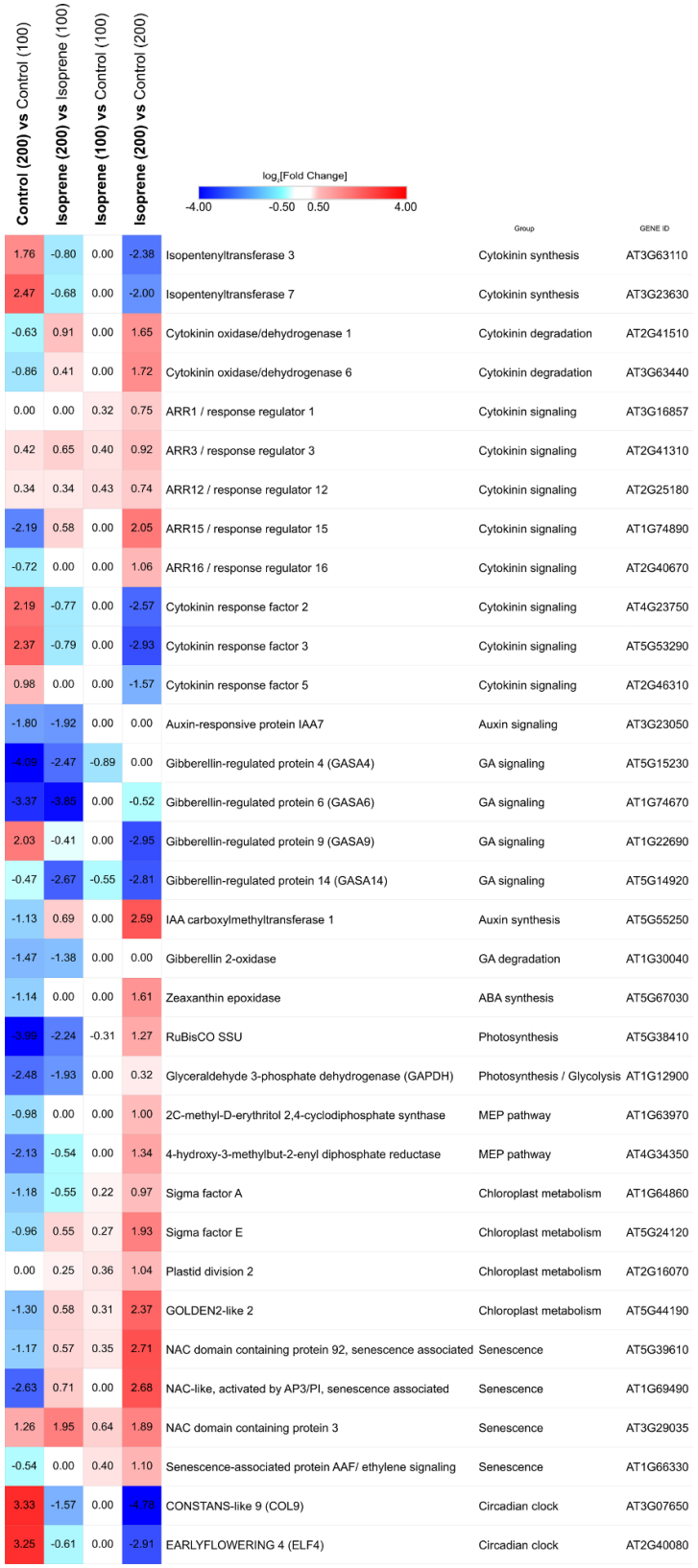
Control (200) vs Control (100)
Isoprene (200) vs Isoprene (100)
Isoprene (100) vs Control (100)
Isoprene (200) vs Control (200)
log2[Fold Change]
-4.00
-0.50
0.50
4.00
Group
GENE ID
1.76 -0.80 0.00 -2.38 Isopentenyltransferase 3 Cytokinin synthesis AT3G63110
2.47 -0.68 0.00 -2.00 Isopentenyltransferase 7 Cytokinin synthesis AT3G23630
-0.63 0.91 0.00 1.65 Cytokinin oxidase/dehydrogenase 1 Cytokinin degradation AT2G41510
-0.86 0.41 0.00 1.72 Cytokinin oxidase/dehydrogenase 6 Cytokinin degradation AT3G63440
0.00 0.00 0.32 0.75 ARR1 / response regulator 1 Cytokinin signaling AT3G16857
0.42 0.65 0.40 0.92 ARR3 / response regulator 3 Cytokinin signaling AT2G41310
0.34 0.34 0.43 0.74 ARR12 / response regulator 12 Cytokinin signaling AT2G25180
-2.19 0.58 0.00 2.05 ARR15 / response regulator 15 Cytokinin signaling AT1G74890
-0.72 0.00 0.00 1.06 ARR16 / response regulator 16 Cytokinin signaling AT2G40670
2.19 -0.77 0.00 -2.57 Cytokinin response factor 2 Cytokinin signaling AT4G23750
2.37 -0.79 0.00 -2.93 Cytokinin response factor 3 Cytokinin signaling AT5G53290
0.98 0.00 0.00 -1.57 Cytokinin response factor 5 Cytokinin signaling AT2G46310
-1.80 -1.92 0.00 0.00 Auxin-responsive protein IAA7 Auxin signaling AT3G23050
-4.09 -2.47 -0.89 0.00 Gibberellin-regulated protein 4 (GASA4) GA signaling AT5G15230
-3.37 -3.85 0.00 -0.52 Gibberellin-regulated protein 6 (GASA6) GA signaling AT1G74670
2.03 -0.41 0.00 -2.95 Gibberellin-regulated protein 9 (GASA9) GA signaling AT1G22690
-0.47 -2.67 -0.55 -2.81 Gibberellin-regulated protein 14 (GASA14) GA signaling AT5G14920
-1.13 0.69 0.00 2.59 IAA carboxylmethyltransferase 1 Auxin synthesis AT5G55250
-1.47 -1.38 0.00 0.00 Gibberellin 2-oxidase GA degradation AT1G30040
-1.14 0.00 0.00 1.61 Zeaxanthin epoxidase ABA synthesis AT5G67030
-3.99 -2.24 -0.31 1.27 RuBisCO SSU Photosynthesis AT5G38410
-2.48 -1.93 0.00 0.32 Glyceraldehyde 3-phosphate dehydrogenase (GAPDH) Photosynthesis / Glycolysis AT1G12900
-0.98 0.00 0.00 1.00 2C-methyl-D-erythritol 2,4-cyclodiphosphate synthase MEP pathway AT1G63970
-2.13 -0.54 0.00 1.34 4-hydroxy-3-methylbut-2-enyl diphosphate reductase MEP pathway AT4G34350
-1.18 -0.55 0.22 0.97 Sigma factor A Chloroplast metabolism AT1G64860
-0.96 0.55 0.27 1.93 Sigma factor E Chloroplast metabolism AT5G24120
0.00 0.25 0.36 1.04 Plastid division 2 Chloroplast metabolism AT2G16070
-1.30 0.58 0.31 2.37 GOLDEN2-like 2 Chloroplast metabolism AT5G44190
-1.17 0.57 0.35 2.71 NAC domain containing protein 92, senescence associated Senescence AT5G39610
-2.63 0.71 0.00 2.68 NAC-like, activated by AP3/PI, senescence associated Senescence AT1G69490
1.26 1.95 0.64 1.89 NAC domain containing protein 3 Senescence AT3G29035
-0.54 0.00 0.40 1.10 Senescence-associated protein AAF/ ethylene signaling Senescence AT1G66330
3.33 -1.57 0.00 -4.79 CONSTANS-like 9 (COL9) Circadian clock AT3G07650
3.25 -0.61 0.00 -2.91 EARLYFLOWERING 4 (ELF4) Circadian clock AT2G40080

Figure 9

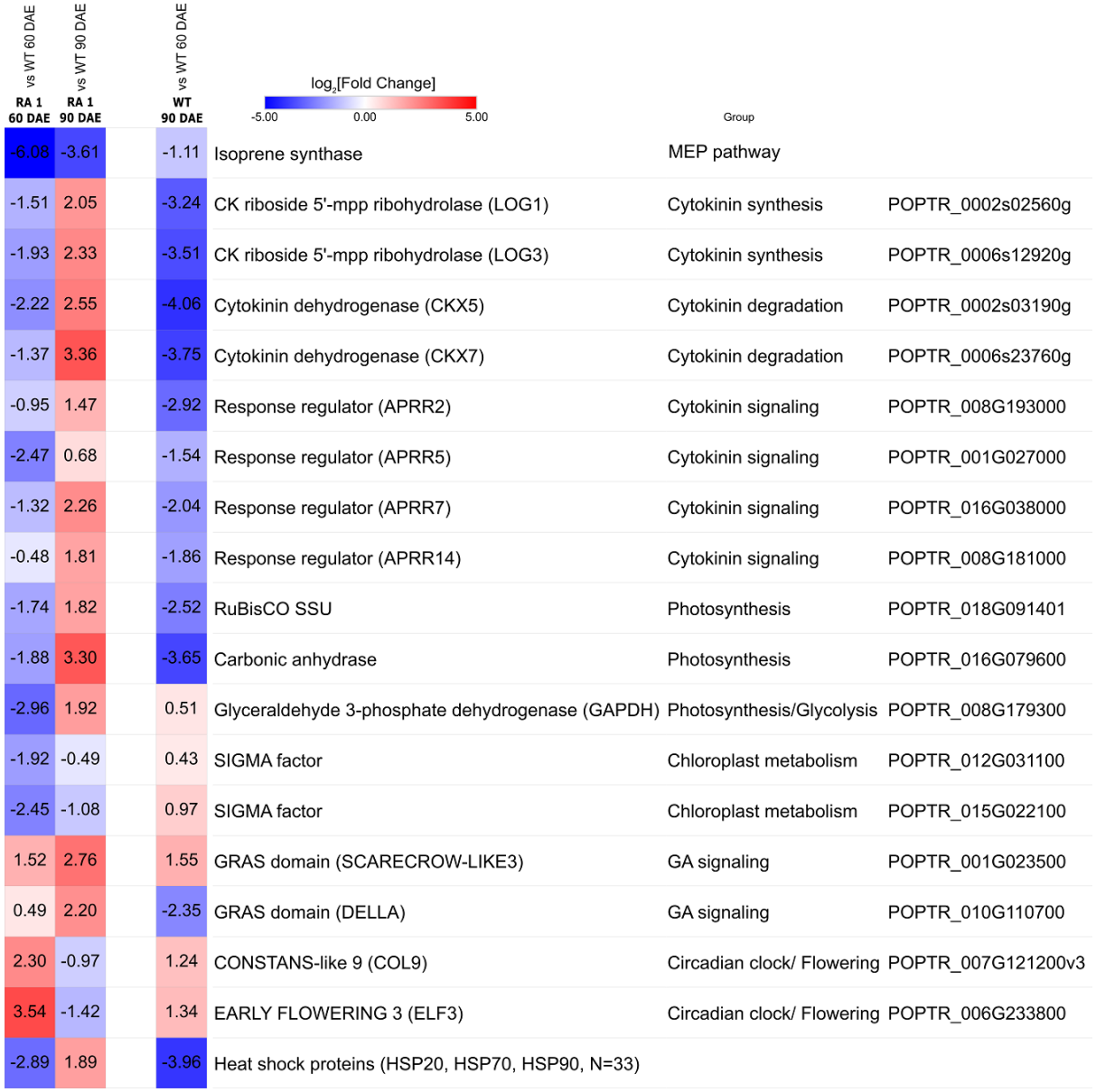

RA 1 60 DAE vs WT 60 DAE	RA 1 90 DAE vs WT 90 DAE	WT 90 DAE vs WT 60 DAE		Group	
-6.08	-3.61	-1.11	Isoprene synthase	MEP pathway	
-1.51	2.05	-3.24	CK riboside 5'-mpp ribohydrolase (LOG1)	Cytokinin synthesis	POPTR_0002s02560g
-1.93	2.33	-3.51	CK riboside 5'-mpp ribohydrolase (LOG3)	Cytokinin synthesis	POPTR_0006s12920g
-2.22	2.55	-4.06	Cytokinin dehydrogenase (CKX5)	Cytokinin degradation	POPTR_0002s03190g
-1.37	3.36	-3.75	Cytokinin dehydrogenase (CKX7)	Cytokinin degradation	POPTR_0006s23760g
-0.95	1.47	-2.92	Response regulator (APRR2)	Cytokinin signaling	POPTR_008G193000
-2.47	0.68	-1.54	Response regulator (APRR5)	Cytokinin signaling	POPTR_001G027000
-1.32	2.26	-2.04	Response regulator (APRR7)	Cytokinin signaling	POPTR_016G038000
-0.48	1.81	-1.86	Response regulator (APRR14)	Cytokinin signaling	POPTR_008G181000
-1.74	1.82	-2.52	RuBisCO SSU	Photosynthesis	POPTR_018G091401
-1.88	3.30	-3.65	Carbonic anhydrase	Photosynthesis	POPTR_016G079600
-2.96	1.92	0.51	Glyceraldehyde 3-phosphate dehydrogenase (GAPDH)	Photosynthesis/Glycolysis	POPTR_008G179300
-1.92	-0.49	0.43	SIGMA factor	Chloroplast metabolism	POPTR_012G031100
-2.45	-1.08	0.97	SIGMA factor	Chloroplast metabolism	POPTR_015G022100
1.52	2.76	1.55	GRAS domain (SCARECROW-LIKE3)	GA signaling	POPTR_001G023500
0.49	2.20	-2.35	GRAS domain (DELLA)	GA signaling	POPTR_010G110700
2.30	-0.97	1.24	CONSTANS-like 9 (COL9)	Circadian clock/ Flowering	POPTR_007G121200v3
3.54	-1.42	1.34	EARLY FLOWERING 3 (ELF3)	Circadian clock/ Flowering	POPTR_006G233800
-2.89	1.89	-3.96	Heat shock proteins (HSP20, HSP70, HSP90, N=33)		

Supplementary Figures and Tables

Isoprene enhances leaf cytokinin metabolism, accelerates growth and induces early-senescence in *Arabidopsis* and *Populus*

Kaidala Ganesha Srikanta Dani[1,6*], Susanna Pollastri[1], Sara Pinosio[2], Michael Reichelt[3], Thomas D Sharkey[4], Jorg-Peter Schnitzler[5], Francesco Loreto[6*]

Table S1. Parameters of LC-MS/MS analysis of cytokinins in positive mode (see methods for details)

Compound	Q1 (m/z)	Q3 (m/z)	Retention Time (min)	DP	CE	CXP	Internal standard
trans-zeatin (tZ)	220.2	136.3	2.4	40	25	16	[$^2H_5$] tZ
tZ-riboside	352.2	220.3	3.4	40	25	30	[$^2H_5$] tZR
trans-zeatin-O-glucoside (tZOG)	382.1	220.2	2.3	40	29	18	[$^2H_5$] tZOG
cZ-riboside	352.2	220.3	3.6	40	25	30	[$^2H_5$] tZR
iPR	336.1	204.3	5.0	40	23	26	[$^2H_6$] iPR
isopentenyl adenine (iP)	204.1	136.0	4.1	40	23	16	[$^2H_6$] iP
tZ-riboside, trans-zeatin riboside, cZ-riboside, cis-zeatin riboside, iPR, isopentenyladenine riboside, DP, declustering potential, CE, collision energy, CXP, collision cell exit potential							

Figure S1

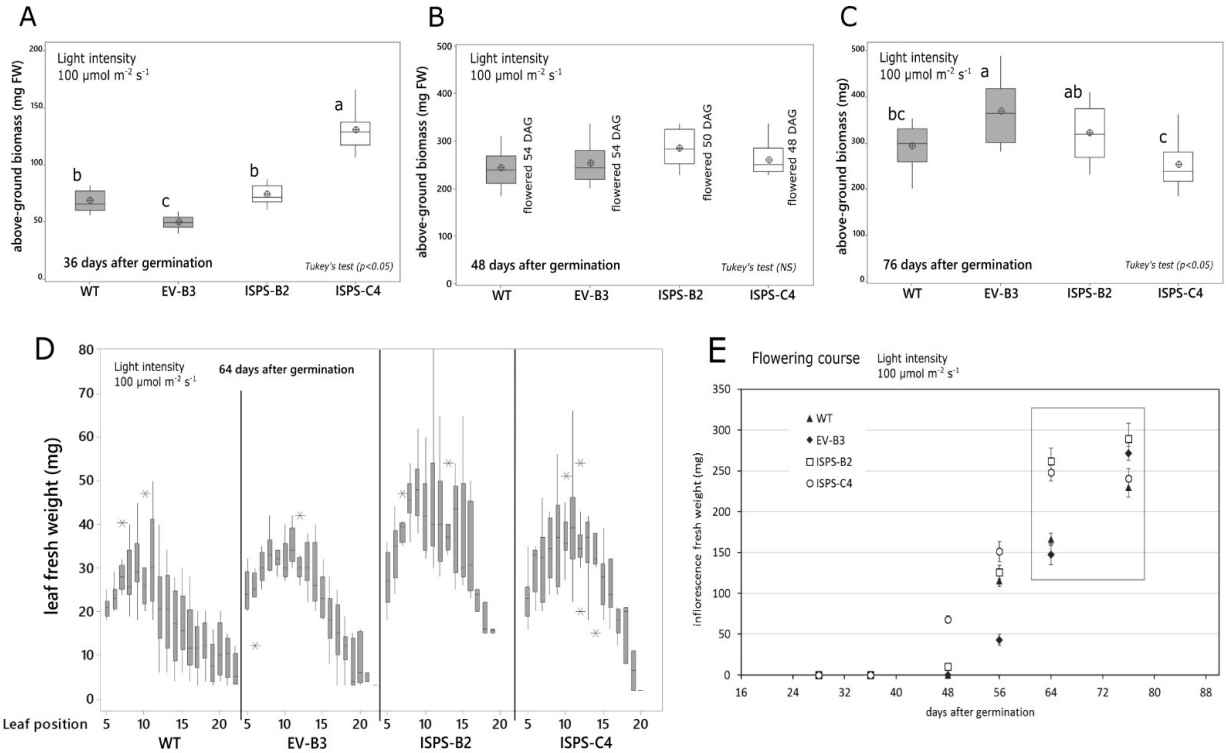

Figure S2

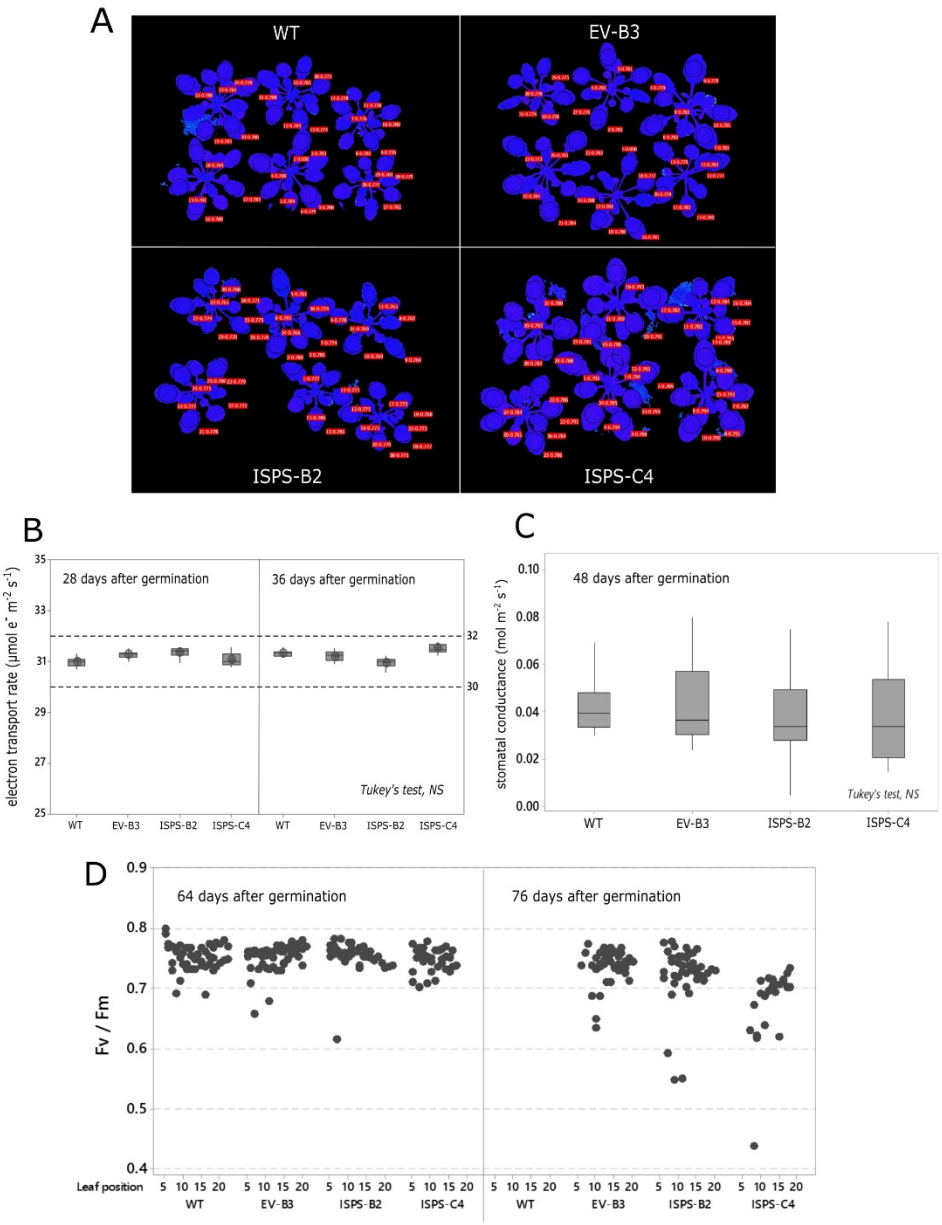
A
WT
EV-B3
ISPS-B2
ISPS-C4
B
28 days after germination
36 days after germination
electron transport rate (µmol e⁻ m⁻² s⁻¹)
Tukey's test, NS
WT
EV-B3
ISPS-B2
ISPS-C4
C
48 days after germination
stomatal conductance (mol m⁻² s⁻¹)
Tukey's test, NS
D
64 days after germination
76 days after germination
Fv / Fm
Leaf position

Figure S3

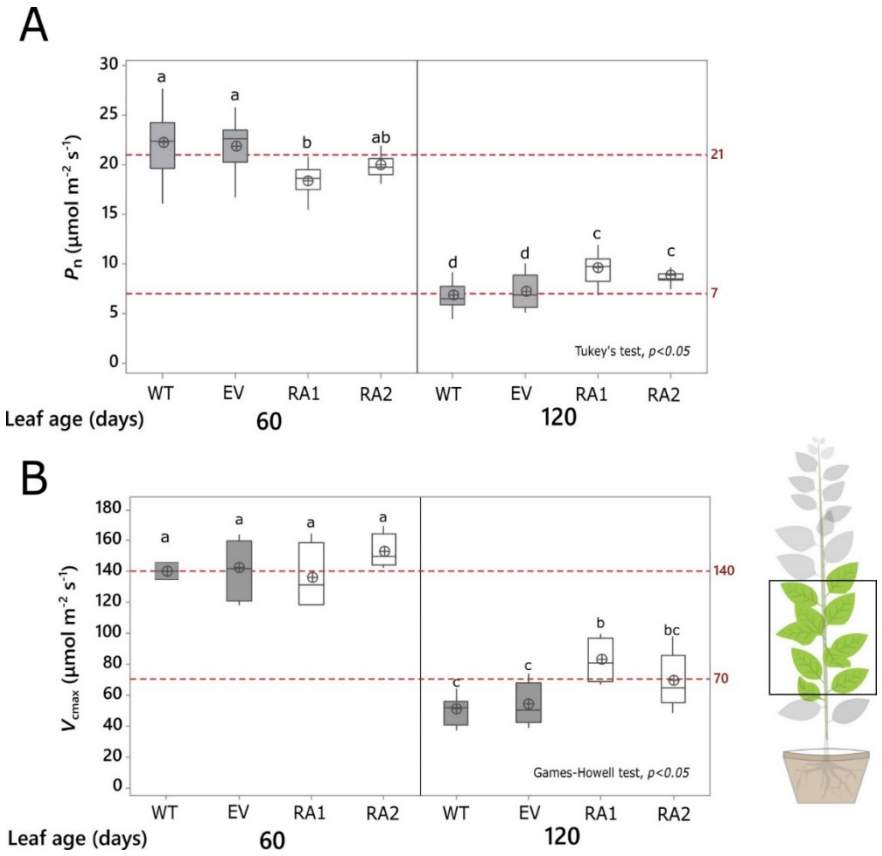
A
P_n (µmol m^{-2} s^{-1})
30
25
20
15
10
5
0
a
a
b
ab
d
d
c
c
21
7
Tukey's test, p<0.05
WT
EV
RA1
RA2
WT
EV
RA1
RA2
Leaf age (days)
60
120
B
V_{cmax} (µmol m^{-2} s^{-1})
180
160
140
120
100
80
60
40
20
0
a
a
a
a
c
c
b
bc
140
70
Games-Howell test, p<0.05
WT
EV
RA1
RA2
WT
EV
RA1
RA2
Leaf age (days)
60
120

Figure S4 (Arabidopsis)